frontiers in Earth Science

ORIGINAL RESEARCH
published: 24 March 2021
doi: 10.3389/feart.2021.640580

Terrestrial Dissolved Organic Matter Mobilized From Eroding Permafrost Controls Microbial Community Composition and Growth in Arctic Coastal Zones

Anders Dalhoff Bruhn[1], Colin A. Stedmon[1], Jérôme Comte[2], Atsushi Matsuoka[3,4], Niek Jesse Speetjens[5], George Tanski[5,6], Jorien E. Vonk[5] and Johanna Sjöstedt[1,7]*

[1] National Institute of Aquatic Resources, Technical University of Denmark, Lyngby, Denmark, [2] Centre - Eau Terre Environnement, Institut National de la Recherche Scientifique, Québec, QC, Canada, [3] Takuvik Joint International Laboratory (CNRS-ULaval), Québec, QC, Canada, [4] Institute for the Study of Earth, Oceans, and Space, University of New Hampshire, Durham, NH, United States, [5] Department for Earth Sciences, Vrije Universiteit Amsterdam, Amsterdam, Netherlands, [6] Permafrost Research Section, Alfred Wegener Institute Helmholtz Centre for Polar and Marine Research, Potsdam, Germany, [7] Department of Biology, Aquatic Ecology, Lund University, Lund, Sweden

OPEN ACCESS

Edited by:
Louise Farquharson, University of Alaska Fairbanks, United States

Reviewed by:
Joanne K. Heslop, German Research Centre for Geosciences, Helmholtz Centre Potsdam, Germany
Alexander Michaud, Bigelow Laboratory for Ocean Sciences, United States
David E. Graham, Oak Ridge National Laboratory (DOE), United States

***Correspondence:**
Anders Dalhoff Bruhn
adbj@aqua.dtu.dk

Specialty section:
This article was submitted to Biogeoscience, a section of the journal Frontiers in Earth Science

Received: *11 December 2020*
Accepted: *24 February 2021*
Published: *24 March 2021*

Citation:
Bruhn AD, Stedmon CA, Comte J, Matsuoka A, Speetjens NJ, Tanski G, Vonk JE and Sjöstedt J (2021) Terrestrial Dissolved Organic Matter Mobilized From Eroding Permafrost Controls Microbial Community Composition and Growth in Arctic Coastal Zones. Front. Earth Sci. 9:640580. doi: 10.3389/feart.2021.640580

Climate warming is accelerating erosion along permafrost-dominated Arctic coasts. This results in the additional supply of organic matter (OM) and nutrients into the coastal zone. In this study we investigate the impact of coastal erosion on the marine microbial community composition and growth rates in the coastal Beaufort Sea. Dissolved organic matter (DOM) derived from three representative glacial deposit types (fluvial, lacustrine, and moraine) along the Yukon coastal plain, Canada, were used as substrate to cultivate marine bacteria using a chemostat setup. Our results show that DOM composition (inferred from UV-Visible spectroscopy) and biodegradability (inferred from DOC concentration, bacterial production and respiration) significantly differ between the three glacial deposit types. DOM derived from fluvial and moraine types show clear terrestrial characteristics with low aromaticity (S_r: 0.63 ± 0.02 and $SUVA_{254}$: 1.65 ± 0.06 L mg C^{-1} m^{-1} & S_r: 0.68 ± 0.01 and $SUVA_{254}$: 1.17 ± 0.06 L mg C^{-1} m^{-1}, respectively) compared to the lacustrine soil type (S_r: 0.71 ± 0.02 and $SUVA_{254}$: 2.15 ± 0.05 L mg C^{-1} m^{-1}). The difference in composition of DOM leads to the development of three different microbial communities. Whereas *Alphaproteobacteria* dominate in fluvial and lacustrine deposit types (67 and 87% relative abundance, respectively), *Gammaproteobacteria* is the most abundant class for moraine deposit type (88% relative abundance). Bacterial growth efficiency (BGE) is 66% for DOM from moraine deposit type, while 13 and 28% for DOM from fluvial and lacustrine deposit types, respectively. The three microbial communities therefore differ strongly in their net effect on DOM utilization depending on the eroded landscape type. The high BGE value for moraine-derived DOM is probably caused by a larger proportion of labile colorless DOM. These results indicate that the substrate controls marine microbial community composition and activities in coastal waters. This suggests that

biogeochemical changes in the Arctic coastal zone will depend on the DOM character of adjacent deposit types, which determine the speed and extent of DOM mineralization and thereby carbon channeling into the microbial food web. We conclude that marine microbes strongly respond to the input of terrestrial DOM released by coastal erosion and that the landscape type differently influence marine microbes.

Keywords: climate change, terrestrial dissolved organic matter, Arctic coastal zone, marine microbial community, chemostat, glacial deposits, permafrost

INTRODUCTION

The permafrost region in the northern hemisphere covers approximately 22% of the land surface which is not covered by glaciers and ice (Obu et al., 2019). A seasonally unfrozen active layer which thaws every year during the warm season is situated on top of the permafrost layer. The permafrost layer itself is permanently frozen, per definition, for at least 2 years in a row (Pollard, 2018). Recent estimates project that ∼1,000 ± 150Pg organic carbon (OC) are stored in the upper 3 m of the soils, plus 500 Pg C in deeper deposits such as yedoma and deltaic sediments (Hugelius et al., 2014; Schuur et al., 2015; McGuire et al., 2018). The amount of carbon stored in active and permafrost layers across the Northern Hemisphere is larger than the carbon storage of any other soil regions on Earth (e.g., temperate and tropical soils) and also surpasses that of the atmosphere (Jobbágy and Jackson, 2000; Strauss et al., 2017).

Due to climate change, permafrost is warming at a global scale (Biskaborn et al., 2019) and the increased loss in soil integrity primes Arctic coastlines for erosion (Günther et al., 2015; Hoque and Pollard, 2016; Obu et al., 2016; Fritz et al., 2017; Couture et al., 2018; Jones et al., 2018). Coastal erosion is further promoted by the reduction in landfast sea ice, making the shores vulnerable to environmental forcing, such as bathing of coastal bluffs in warm seawater and increased wave heights during storms (Overeem et al., 2011; Fritz et al., 2017). Dissolved organic matter (DOM), which is mobilized from permafrost compartments in Cryosols (i.e., soil type in cold regions which is affected by permafrost and cryoturbation processes), is highly biodegradable and directly available for microbial utilization upon permafrost thaw (Dou et al., 2008; Vonk et al., 2013; Abbott et al., 2014; Drake et al., 2015; Fritz et al., 2015; Spencer et al., 2015; Wologo et al., 2020). Increased release of DOM from degrading permafrost landscapes to the Arctic coastal zone (ACZ) can potentially lead to changes in OC processing by marine microbes (Colatriano et al., 2018). This can in turn influence marine primary production and higher trophic levels by increases in regenerated nutrients (Sipler et al., 2017), competition for mineral nutrients (Thingstad et al., 2008) and decreased light penetration (Arrigo and Brown, 1996). Utilization of dissolved organic carbon (DOC) (Tanski et al., 2019) and its offshore transport to deeper oceans (Belicka et al., 2002) will also be affected by the change in microbial carbon processing. This will ultimately affect the overall carbon cycle and thereby impact the carbon budget and aquatic ecosystems in the ACZ. Due to the magnitude of permafrost thaw (Romanovsky et al., 2010; Smith et al., 2010) and increase in coastal erosion (Günther et al., 2015; Fritz et al., 2017; Jones et al., 2018) a better estimate of marine microbial carbon processing of DOC from coastal erosion and its effect on microbial communities in ACZ is needed.

In this study we examine three different permafrost landscape units, which are omnipresent in our study region (Yukon coastal plain, western Canadian Arctic). The landscape units differ from their (post-)glacial genesis and OC storage and include fluvial (FLU) deposits (∼53 kg OC m^{-3} in the top meter of soil); lacustrine (LAC) deposits (∼47 kg OC m^{-3}); and moraine (MOR) deposits (∼40 kg OC m^{-3}) (Couture et al., 2018). Organic matter in FLU deposits comes from dispersed plant detritus mixed with mineral soil or peat layers that accumulated under stagnant water conditions in abandoned river channels (Rampton, 1982; Schirrmeister et al., 2011). Organic matter in LAC deposits was incorporated from the reworking and deposition of older material eroded from shore bluffs into lakes together with *in situ* production of fresh OM from aquatic plants and animals (Schirrmeister et al., 2011) along with talik formation (Wolter et al., 2017) and OC degradation in these lake sediments (Walter Anthony et al., 2018) due to permafrost thaw under the lakes. For the MOR deposit type, peat lenses and organic-rich silt is characteristic for the upper part of the deposits, where syngenetic formation and cryoturbation of permafrost has been the main driver behind the storage of OM (Rampton, 1982). This lead to high rates of accumulation and preservation of plant remains, which consists of less decomposed OM and high TOC (Schirrmeister et al., 2011). The organic matter incorporated into FLU and LAC has likely experienced Holocene decomposition since they were waterlogged during this period, whereas MOR likely been preserved since the Pleistocene and experienced very low decomposition (Strauss et al., 2017). During Holocene decomposition, labile OM, such as aliphatic and peptide-like compounds, in FLU and LAC deposits have been reworked by microbial activity, thereby leaving a higher amount of less labile compounds, such as aromatic compounds, when refrozen during the cooling of the middle Holocene (Stapel et al., 2017; Strauss et al., 2017; Heslop et al., 2019).

Terrestrial OM along permafrost coasts is released primarily as particulate organic carbon (POC) to the ACZ (Tanski et al., 2016). Although erosion of the coastline delivers relatively low amounts of DOC (annual flux of 55 Mg yr^{-1}) to the ACZ compared to Arctic rivers (34–38 Tg y^{-1} if the entire pan-Arctic watershed is considered) (Guo and Macdonald, 2006; Holmes et al., 2012; Tanski et al., 2016; Wild et al., 2019), the DOC

released by coastal erosion is highly biodegradable upon thaw (Vonk et al., 2013, 2015; Fritz et al., 2015; Spencer et al., 2015). In addition, upon exposure to seawater with high ionic strengths, ion exchange can release and further dissolve mineral-bound particulate OM or colloids, which can mobilize 19–50% of the bound OM (Kaiser and Guggenberger, 2000; Kawahigashi et al., 2006; Dou et al., 2008). The release of DOM from coastal erosion can therefore be assumed to have a large influence on microbes in coastal environments. Multiple studies have shown that the supply of permafrost-derived DOM can lead to rapid changes in marine microbial community composition and growth (Blanchet et al., 2017; Sipler et al., 2017; Müller et al., 2018) and it has recently been shown that the marine bacteria *Chloroflexi*, have the capacity to utilize terrestrial DOM (Colatriano et al., 2018). The effect of rapid mineralization of OC from permafrost thaw has been shown for freshwater bacterial communities, where microbes can degrade 34% of permafrost-derived DOC within 14 days of incubation (Vonk et al., 2013) or 47% within 28 days of incubation (Mann et al., 2015). However, there are knowledge gaps associated with the impact of DOM derived from coastal erosion of different glacial deposit types and how it affects marine microbial composition and carbon processing.

Here we study the bioavailability of DOM, released directly to marine microbes in the ACZ, through coastal erosion, using a chemostat approach. This allows the development of a stable microbial community under conditions where the constant supply of substrate could reflect conditions in coastal waters influenced by coastal erosion. We investigate the biodegradability of DOM derived from three representative glacial deposit types (FLU, LAC, and MOR) to test if differences in DOM character can induce differences in bacterial community composition (BCC) and bacterial growth efficiency (BGE). We also follow the changes in DOM character imparted by microbes using absorbance and fluorescence spectroscopy. We hypothesized that (i) the DOM provided by erosion of permafrost coasts is highly bioavailable for marine microbes and that (ii) different DOM characteristics among glacial deposit types induce different growth rates and the establishment of different bacterial communities.

MATERIALS AND METHODS

Study Area

The study area is located in the western Canadian Arctic on the Yukon coastal plain near Herschel Island - Qikiqtaruk (**Figure 1**). The Yukon coastal plain is about 282 km long and 10–30 km wide. Cliff heights are diverse, ranging from 2–3 m on the mainland across from Herschel Island to 60 m in the eastern part of the Yukon coastal plains (Couture et al., 2018). The mean annual air temperature is −11°C, with the highest temperature during July month reaching 7.8°C (1971–2000) (Environment Canada, 2016). The parent material of the Cryosols in the Yukon coastal plains originate from an ice-rich glacial margin and has been deposited by glacial transportation (ice and meltwater) of earth material and later on reworked by water during Holocene Thermal Maximum (higher than modern summer temperatures) (Fritz et al., 2012).

Sampling targeted fluvial, lacustrine, and moraine deposits since they represent the permafrost landscape on the Yukon coastal plain and differ the most in OC content and storage among all post-glacial landscape units (Couture et al., 2018). Fluvial sediments are poorly-drained floodplain deposits consisting of fine-grained sediments. The fluvial sediments used for this study were taken from the floodplains of the Babbage River Delta and may resemble other floodplain deposits in the study area. The fine-grained and ice-rich fluvial deposits are prone to erosion and can be mobilized with increasing river discharge, floods and deltaic or river bank erosion. Lacustrine sediments originate from thermokarst formation within moraine deposits (Krzic et al., 2010). These sediments accumulated with lake formation and have a fine-grained composition with peat layers present (Rampton, 1982). Lacustrine deposits are situated in flat and gently sloping terrain and have a poor surface drainage (Rampton, 1982). Moraine deposits are very common and cover approximately 50% of the formerly glaciated part of the Yukon coastal plain. Moraines are ice-rich and surfaces usually well drained due to a distinct topographic gradient with slopes of 5–25° (Rampton, 1982). The finer sediments in the upper layer of moraine soil were commonly washed away by meltwater from the glacier and moved to lacustrine and marine environments (Krzic et al., 2010).

Collection of Samples

Permafrost and active layer sediment samples as well as coastal seawater samples were collected in April and May 2019. The sediment samples were taken with a SIPRE corer at three sites with different glacial deposit types; (A) fluvial (FLU, fluvial deposits, 69.20686 N, 138.36730W), (B) lacustrine (LAC, lacustrine-wetland deposits, 69.33580 N, 138.8768W), and (C) moraine (MOR, moraine ridge-drained deposits, 69.46122N, 139.24230W). Subsamples were taken from the active layer (FLU: 9–24 cm, LAC: 4–14 cm, and MOR: 27–42 cm) and from the permafrost layer (FLU: 105–120 cm, LAC: 55–70 cm, and MOR: 90–105 cm) of the cores. All samples were stored frozen (−18°C) and in the dark.

Seawater samples were collected in the wider Mackenzie Bay in Herschel Basin through the sea ice using a Niskin water sampler (69.50978 N, 138.86278 W). A Conductivity, Temperature, and Depth (CTD) cast was taken to make sure seawater was collected from the main water body avoiding layers below the sea ice or close to the seabed. Seawater was stored in pre-leached 1 L Nalgene bottles, which were rinsed with the sample two to three times. Seawater was stored cold (4°C) in the dark for 1 month prior to the experiment. The seawater had a salinity of 31 ppt and was later used as a bacterial inoculum.

Preparation of Soil Medium and Bacterial Culture

All the equipment used in the experiment was acid cleaned. Soil extracts were prepared from the six soil cores from FLU, MOR, and LAC glacial deposit types. For each glacial deposit type, extracts were prepared by dissolving soils from the active layer (wet weight; FLU: 343 g, LAC: 331 g, and MOR: 282 g)

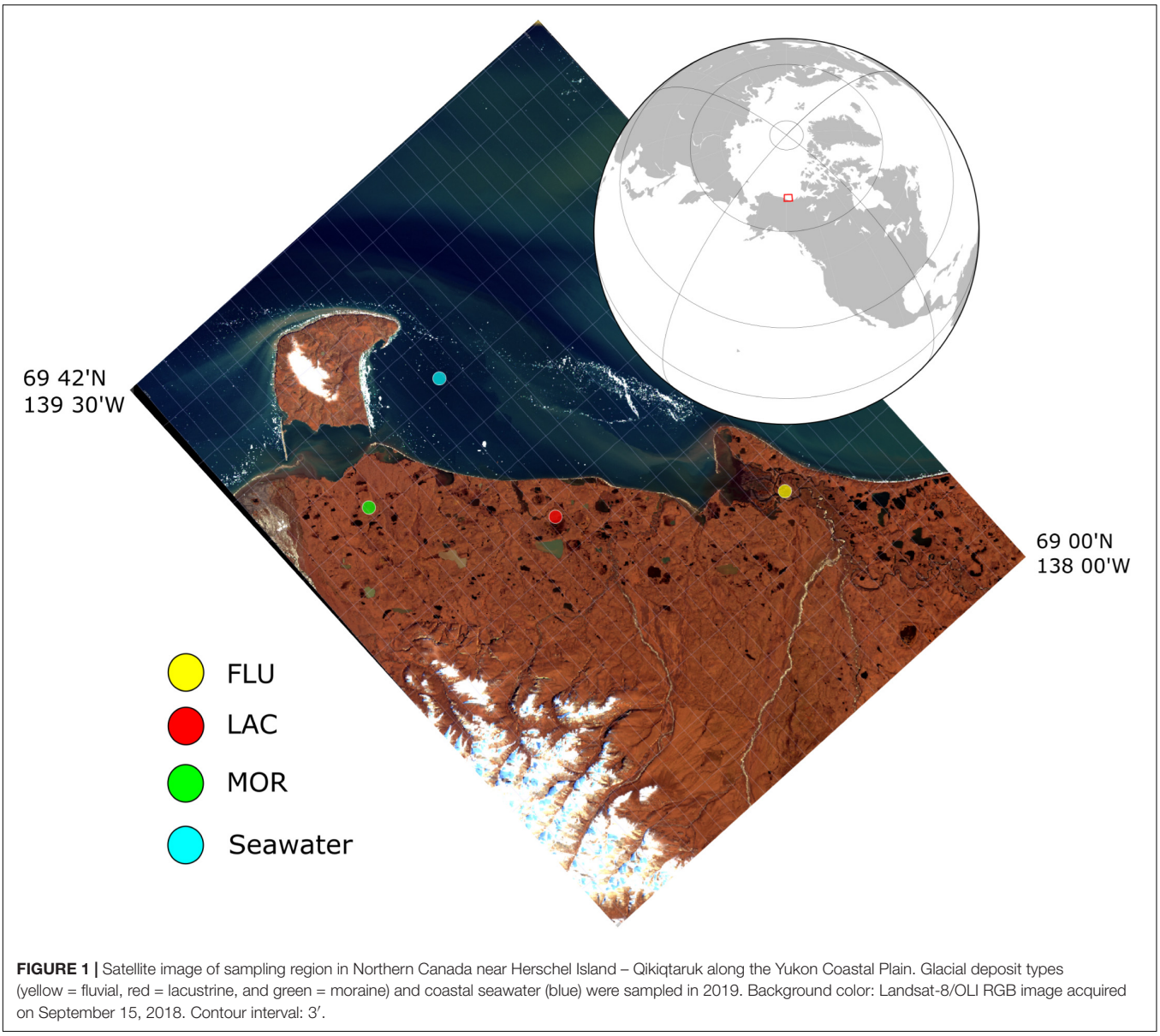

FIGURE 1 | Satellite image of sampling region in Northern Canada near Herschel Island – Qikiqtaruk along the Yukon Coastal Plain. Glacial deposit types (yellow = fluvial, red = lacustrine, and green = moraine) and coastal seawater (blue) were sampled in 2019. Background color: Landsat-8/OLI RGB image acquired on September 15, 2018. Contour interval: 3′.

or the permafrost layer (wet weight; FLU: 581 g, LAC: 192 g, and MOR: 222 g) separately into 8 L of ultrapure water (water extraction). The same volume of soil was added, which resulted in different mass due to differences in ice content between the glacial deposit types. The soil was kept in suspension overnight and then allowed to settle for 1 h before filtration through a 0.2 μm filter (AcroPak Capsules with Supor® Membrane, PALL). Salts were added (NaCl 21.1 g, $MgCl_2$ 4.5 g, Na_2SO_4 3.5 g, $CaCl_2$ 1 g, KCl 0.6 g, KBr 0.1 g, H_3BO_3 0.02 g, and $NaHCO_3$ 0.2 g per L) to a final salinity of 31 ppt (reflecting the same salinity and ratios as the sampled seawater). The water extractions from the soils were then stored at 20°C overnight to let the salts completely dissolve. For each glacial deposit type, the soil extract from the active layer was mixed with an equal volume of soil extract from the permafrost layer (2 × 7 L mixed soil extracts per glacial deposit type) and then autoclaved. We mixed the two layers to reflect what will happen during coastal erosion when the whole soil column collapses into the ACZ. After the first autoclaving, the mixed soil extracts were split into four replicates (4 × 3.5 L mixed soil extracts per deposit type). The extracts were then re-filtered through a 0.2 μm filter and KNO_3 and K_3PO_4 was added to a final concentration of 16 and 1 μM, respectively. The sterile soil extracts were then autoclaved a second time. The sterile soil extracts were stored overnight, in darkness at 4°C, until the start of the experiment, where they were used as medium for the chemostat cultures. The mixed and sterile soil extracts are hereafter referred to as medium/media.

The sampled seawater obtained from Herschel Basin was used as bacterial inoculum. To adapt the marine microbial communities to the DOM derived from the Cryosols and thereby get a faster establishment in the chemostats, 900 ml of seawater

was mixed with 200 ml from the respective autoclaved medium, 3 days before the start of each chemostat experiment. This formed the base of the culture to be used in the chemostat experiments.

Experimental Setup

Chemostats for each glacial deposit type were run in quadruplicates using the same approach as reported in Sjöstedt et al. (2012b). For each chemostat, 3.5 L of medium was used and 0.2 L of marine bacterial inoculum as culture. Medium was fed dropwise through a glass tube to prevent back growth (Hagstrom et al., 1984). Oxygen was supplied by passing air through a 0.2 μm pore-size polytetrafluoroethylene Acrodisc CR filter (Pall Corporation) (Zweifel et al., 1996). The chemostats were run for 14 days in the dark and at 20°C, which is standard temperature for biodegradation experiments (Vonk et al., 2015). The dilution rate was 1 day^{-1}, which is close to the median growth rate of marine bacteria ranging from polar to temperate regions (Moriarty, 1986).

Samples for bacterial abundance (BA) and optical measurements of DOM (absorbance and fluorescence) were taken both from the culture (once per day) and the medium (every 2 days). Bacterial community composition samples were taken from the culture every day. Samples for DOC and nutrient concentrations were taken from the culture daily and from the medium at day 0, 7 and 14. Samples from the culture were taken from the outflow of the chemostat, whereas samples from the medium were taken by carefully disconnecting the tubing feeding the culture with medium.

DOM Absorbance and Fluorescence

Samples (20 ml) were collected in acid washed and precombusted 40 ml glass vials with Teflon-lined caps and measured within 2 h of collection. The absorption spectrum of colored DOM (CDOM) and excitation-emission-matrix (EEM) of fluorescent DOM (FDOM) were measured on filtered samples (0.2 μm Supor Acrodisc, Pall Corporation). Both CDOM and FDOM was measured on an Aqualog fluorometer (HORIBA Jobin Yvon). The CDOM absorbance was measured in a 1 cm quartz cuvette between 239 and 800 nm, with increment of 3 nm and integration time of 0.1 s. The FDOM fluorescence was measured in the same 1 cm quartz cuvette immediately after the CDOM measurement. Emission wavelengths were 245–824 nm with increment of 2 nm and excitation wavelengths 240–450 nm with increment of 5 nm. The emission integration time was adjusted to account for varying FDOM fluorescence intensities between samples. An ultrapure water sample was used as a blank for both absorbance and fluorescence measurements.

The absorption spectrum of the ultrapure blank was subtracted from the absorption spectrum of the chemostat samples. This was performed by subtracting the absorption mean value between 590 and 800 nm. The absorption values were converted to the naperian absorption coefficient according to the following equation, $a_\lambda = 2.303^*A/L$, where A (unitless) is the optical density measured by the instrument and L (m) is the length of the cuvette and λ is wavelength. Fluorescence data was converted into Raman units (R.U) applying Raman calibration (Lawaetz and Stedmon, 2009), blank subtracted and then corrected for inner filter effects using the drEEM toolbox (Murphy et al., 2013). The quality of CDOM in the contrasting media were compared by using the spectral slope coefficients (Helms et al., 2008) and the carbon specific UV absorbance at 254 nm, $SUVA_{254}$ (based on decadic absorbance) (Weishaar et al., 2003). The intensity of CDOM absorption in the media and the cultures was compared using the absorption at 330 nm (highest observed degradation wavelength). The fluorescence intensities were summarized using the peak regions defined by Coble (1996). An attempt to characterize the fluorescence data using parallel factor analysis was unsuccessful. A robust result could not be obtained largely due to the fact that the changes in fluorescence occurring were very minor and that the sample dataset largely represented replicate samples of same medium, which invalidated the use of the commonly applied split half analysis for testing the result.

The steady state period for the cultures were determined based on achievement of a stable CDOM absorbance signal (330 nm) after initial flushing and establishment of the cultures during the first week (between days 7 and 13, **Supplementary Figure 1**).

DOC and Nutrients

After filtration, subsamples for DOC, total dissolved nitrogen (TDN), nitrate/nitrite and phosphate were collected in 30 mL acid-washed HDPE bottles and stored at −20°C until analysis. DOC and TDN concentrations were determined by high-temperature combustion (720°C) using a Shimadzu TOC-V CPH-TN carbon and nitrogen analyzer. The instrument was calibrated using acetanilide (Cauwet, 1999) and carbon determination was referenced to the community deep-sea reference (Hansell laboratory, Miami). DOC accuracy was assured by comparing to reference material provided by the Hansell Laboratory (Sargasso Sea water from 2,600 m near Bermuda; DOC concentration of 42–44 μM). Precision was estimated using a (more comparable) higher concentration sample of aged seawater. This was analyzed every 8 samples in the runs, and was determined to be ±7 μM. Nitrite, nitrate and phosphate were analyzed on a SmartChem200 discrete analyzer (AMS Alliance). The combined concentration of nitrate and nitrite was determined using the method described in Schnetger and Lehners (2014). Phosphate was measured using the manual method described in Hansen and Koroleff (1999). Nutrients standard kits from OSIL were used for calibration.

Bacterial Abundance

Samples (1.6 ml) for BA were fixed with glutaraldehyde (1% final conc.) and stored at −20°C until measured in the flow cytometer. Samples were stained with SybrGreen (Invitrogen) and cells were counted on a FACSCantoII flow cytometer (BD Biosciences), as previously described (Gasol and Del Giorgio, 2000). Fluorescent beads (BD Trucount Tubes, BD Biosciences) were used to calibrate the flow rate. The data was processed using FlowJo9.9.5. Average bacterial abundances were calculated for the steady state period (days 7–13). Bacterial carbon production

(BCP) was calculated based on the bacterial abundance as cells produced per day multiplied by a carbon constant ($1.6^{*}10^{-15}$ moles carbon $cell^{-1}$ (Lee and Fuhrman, 1987).

Bacterial Community Composition

Samples for BCC analysis were taken from the cultures from each deposit type every day. 100 ml of water was filtered through 0.2 μm Supor filters (25 mm; Pall Corporation) to collect bacterial biomass for DNA extraction. The filters were stored at −20°C until extraction. The samples from days 0, 9, 11, and 13 for each culture was selected for analysis. From these filters, DNA was extracted using the Qiagen Power Soil kit.

Amplification of the 16S rRNA gene, equimolar pooling and sequencing was performed at the Plateforme d'analyses génomiques (IBIS, Université Laval, Quebec City, QC, Canada). Amplification of the 16S V3–V4 regions was performed using the sequence specific regions (341F-805R) described in Herlemann et al. (2011) using a two-step dual-index PCR approach specifically designed for Illumina instruments. In the first step, the gene specific sequence is fused to the Illumina TruSeq sequencing primers and PCR was carried out in a total volume of 25 μL that contains 1× Q5 buffer (NEB), 0.25 μM of each primer, 200 μM of each dNTPs, 1 U of Q5 High-Fidelity DNA polymerase (NEB) and 1 μL of template DNA. The PCR started with an initial denaturation at 98°C for 30 s followed by 35 cycles of denaturation at 98°C for 10 s, annealing at 55°C for 10 s, extension at 72°C for 30 s and a final extension at 72°C for 2 min. The PCR reaction was purified using the Axygen PCR cleanup kit (Axygen). Quality of the purified PCR products was checked on a 1% agarose gel. A 50–100 fold dilution of this purified product was used as a template for a second PCR step with the goal of adding barcodes (dual-indexed) and missing sequence required for Illumina sequencing. Cycling for the second PCR were identical to the first PCR but with 12 cycles. PCR reactions were purified as above, checked for quality on a DNA7500 Bioanlayzer chip (Agilent) and then quantified spectrophotometrically with the Nanodrop 1000 (Thermo Fisher Scientific). Barcoded amplicons were pooled in equimolar concentration for sequencing on the Illumina Miseq.

Quality control of the sequences was performed by first removing the primer sequence using the Cutadapt 2.7 tool (Martin, 2011) and secondly by trimming the sequences at 260 bp (forward sequence) and 190 bp (reverse sequence). Sequence analysis was then performed using the IBIS computing infrastructure and the Dada2 algorithm (Callahan et al., 2016). In the end, 1,694,984 sequences were retained (median of 42,939 sequences per sample) following the different quality filters resulting in a total of 912 amplicon sequence variants (ASV). Taxonomic assignment was performed using the SILVA database (v.138) (Quast et al., 2013). DNA sequences have been deposited in the National Centre for Biotechnology Information (NCBI) Sequence Read Archive under accession number PRJNA675030.

A statistical method applied for differential gene expressions was used to rank ASVs consistently present in replicates as representative for each deposit type (Robinson and Smyth, 2008). In brief, a tagwise dispersion function [edgeR, R package (Robinson et al., 2010)] was used to rank ASVs according to their consistency among replicates and analyze which ASVs that differed significantly between deposit types. Differences were considered significant at $p < 0.01$. By using a generalized linear model, we tested for differential representation of ASVs between deposit types using the Toptag function, an analysis quite similar to an ANOVA. The analysis applies $\log_2$-counts per million (logCPM) that is used for estimating relative representation in the community, where low value within a range from 1 to 100 is considered high relative abundance. The analysis also reports logFC that is the x-fold change in ASV contribution to the community. The change in $\log_2$ CPM gives a measure of the consistency of replicates (Canelhas et al., 2016).

Richness (S.Obs, observed number of species) and evenness were calculated in R 3.0.2 using the package Vegan (Oksanen et al., 2019). Non-metric multidimensional scaling (NMDS) was performed using normalized data (relative abundances) of ASVs obtained from sequencing of the 16S rRNA gene. Distances were based on Bray–Curtis dissimilarity matrix to describe relationships in community composition among samples. Vectors representing significantly correlated (PERMANOVA, $p \leq 0.05$, df = 39, n = 999 permutations) DOM characteristics were plotted with the ordination [R 3.0.2, Vegan package (Oksanen et al., 2019)]. Vector length and direction reflects strength and direction of correlation between the DOM characteristics and community composition. Correlations between differences in community composition and differences in DOM utilization (BCP, BGE, and change in DOM characteristics between medium and culture) was investigated using Mantel tests [R 3.0.2, mvabund package, (Wang et al., 2012)].

Biological Oxygen Demand (BOD)

To investigate respiration rates, a sample from each culture replicate in each glacial deposit type (n = 12) was taken at the end of the experiment and incubated for 24 h. Oxygen consumption was measured using a Pyroscience Firesting four channel optode oxygen sensor equipped with 20 mL respiration vials and a temperature sensor. As the chemostats for each glacial deposit type were set up sequentially (1 day apart), the respiration measurements could all be carried out on day 13 (steady state period). Medium and culture from each glacial deposit type was mixed 1:1, to ensure adequate substrate supply during the respiration measurements. Respiration rates were calculated as the slope of oxygen concentration over time for two periods (2–12 h and 12–24 h) as for several of the incubations it was clear that there was a shift (flattening) of the oxygen concentrations during the BOD experiment. Data from the first 2 h were disregarded as it was clear there was a lag time before the establishment of stable respiration rates.

Data Analysis, Presentation, and Statistics

To simplify the data analysis only measurements from the steady state period were used to compare the growth and uptake rates of the cultures. For the optical measurements (absorption and fluorescence), the absorption spectrum and the EEM from the

culture were subtracted with the absorption spectrum and the EEM from their respective medium for each day in the steady state period. The newly created absorption spectra and EEMs from the subtraction could then be used to identify the net production or removal of CDOM and FDOM. A mean value per deposit type was calculated using replicates and days in the steady state.

To investigate the fate of bioavailable carbon from the glacial deposit types, four parameters were calculated; (1) total respiration (calculated from BOD experiments as the sum of respiration rates <12 h and >12 h multiplied by 12 h), (2) total bacterial carbon production [based on bacterial abundance as cells produced per day multiplied by a carbon constant of $1.6*10^{-15}$ moles carbon $cell^{-1}$ (Lee and Fuhrman, 1987)], (3) the total change in DOC concentration (calculated from the difference between medium and culture) and (4) BGE (calculated by dividing BCP by the DOC uptake).

In order to test for differences between glacial deposit types an analysis of variance (ANOVA) test was performed when criteria of normality and heterogeneity was met. If these criteria were not met, the Kruskal–Wallis test was applied. To resolve regions of the absorption spectra and fluorescence EEMs where medium and culture differed significantly, a two sample *t*-test was applied for each wavelength independently. The significance level was set to a *p*-value of 0.05. ANOVA and *t*-test ran in MatLab while Kruskal–Wallis test was applied in R.

The averages (mean) and standard deviations were calculated across the four replicates within each glacial deposit type. This was applied to all parameters using all measurements in the steady state (across days and replicates) unless else stated. Difference in samples number are due to missing data and outliers (defined from boxplots in R) and sample numbers will be stated after each parameter for each glacial deposit type.

RESULTS

Characteristics of DOM

The DOC concentration in the media was highest in LAC, followed by MOR and FLU with an average concentration of 632 (±34, $n = 8$), 543 (±36, $n = 8$), and 526 (±26, $n = 6$) μM DOC, respectively (**Figure 2**). DOC concentrations in the LAC medium were significantly higher than in both the MOR and FLU medium (ANOVA, $p < 0.01$), while MOR and FLU were not significantly different (ANOVA, $p = 0.16$). One replicate of FLU (2 out of 8 measurements) was removed when calculating the mean DOC concentration due to its anomalously low value (368 μM), while the source of the error could not be identified. The average DON concentration in the media was 28.7 (±4.5, $n = 8$), 25.2 (±1.9, $n = 8$), and 24.1 (±2.7, $n = 8$) μM DON for FLU, LAC, and MOR, respectively (**Figure 2**) and there was no significant difference among the three media (ANOVA, $p > 0.05$). The DOC:DON ratios for FLU, LAC, and MOR media were 17.0 (±1.2, $n = 8$), 25.1 (±1.4, $n = 8$), and 22.8 (±2.7, $n = 8$), respectively. The DOC:DON ratio for FLU was found to be significantly lower than those of LAC and MOR (ANOVA, $p < 0.01$), while LAC and MOR did not differ significantly between each other (ANOVA, $p > 0.05$).

The LAC medium had the highest absorption coefficients (**Figure 3**). The absorption coefficients values at 330 nm differed significantly between all three media and were 15.5 m^{-1} (±0.4, $n = 8$) for LAC, 9.2 m^{-1} (±0.5, $n = 12$) for FLU, and 7.3 m^{-1} (±0.5, $n = 11$) for MOR (**Figure 3**, ANOVA, $p < 0.01$). Spectral slopes (S) and $SUVA_{254}$ were used to assess the quality of the CDOM (**Table 1**). The S values for 275–295 nm (UVB) and 350–400 nm (UVA) ranged between 13.4–13.7 and 19.2–21.3 μm^{-1} in the three media. The spectral slopes for the UVB area did not differ significantly between the three media (ANOVA, $p > 0.05$), while the spectral slope of the UVA area was significantly higher in FLU medium than in the other two media (ANOVA, and $p < 0.05$). The spectral slope ratio (S_r) values differed significantly between all media (ANOVA, $p < 0.01$) and were highest for LAC followed by MOR and FLU. The $SUVA_{254}$ values (**Table 1**) were also significantly different between all media (ANOVA, $p < 0.01$) and were highest for LAC, followed by FLU and MOR.

The fluorescence characteristics of the media are shown in **Figure 3** and the fluorescence intensities for common peak regions (Coble, 1996) are reported in **Table 1**. As with the absorption spectra, the fluorescence intensities differed between the media. The visible wavelength peaks (peak A, C, and M) were significantly different between all media (ANOVA, $p < 0.01$) with highest values for LAC, followed by FLU and MOR (**Table 1**). For peak T, the fluorescence intensities did not differ between FLU and LAC (ANOVA, $p > 0.05$), while it was significantly lower for MOR compared to the other two (ANOVA, $p < 0.01$) (**Table 1**). For peak B the fluorescence intensities did not differ significantly between MOR and LAC (ANOVA, $p > 0.05$), while FLU had significantly higher intensity than the other two (ANOVA, $p < 0.01$) (**Table 1**).

Alteration of DOM in the Cultures

Inorganic nutrients were added to ensure replete conditions and carbon limitation in the chemostats. Measured nutrient concentrations in the media were on average 13–15 μM for combined nitrate and nitrite and 0.68–1.01 for phosphate, and remained above 6 and 0.3 μM, respectively in the water flowing out of the cultures.

There were a significant difference in the concentrations of DOC and DON between the medium and the culture for all glacial deposit types (ANOVA, $p < 0.05$). The total removal of DOC in FLU, LAC, and MOR cultures was 132 (±50, $n = 28$), 160 (±46, $n = 28$), and 158 (±48, $n = 28$) μM (**Table 2**) corresponding to 24% (±9%), 25% (±7%), and 29% (±8%) of the initial DOC, respectively. For DON, the highest removal was instead observed for FLU culture and was found to be 10 (±4, $n = 28$) μM corresponding to 36% (±8%) loss, whereas for LAC and MOR cultures it was found to be 4 (±2, $n = 28$) and 4 (±1, $n = 28$) μM corresponding to a loss of 17% (±6%) and 18% (±3%) respectively. The DOC:DON ratios in the cultures changed from their corresponding media and were calculated to be 22 (±4.5, $n = 28$), 22.6 (±1.9, $n = 28$) and 20.8 (±6.2, $n = 28$) for respectively FLU, LAC, and MOR cultures, however, the change was only found to be significant for the FLU deposit type (ANOVA, $p < 0.01$).

The change in the absorption spectra (**Figure 4**) reveals the spectral fingerprint on the CDOM imparted by the

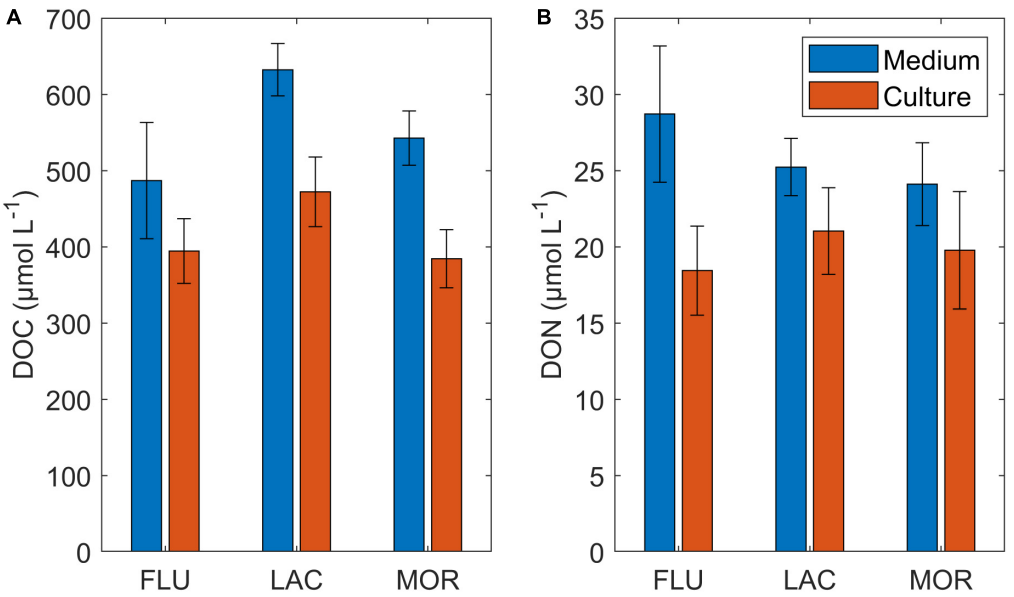

FIGURE 2 | Average DOC **(A)** and DON **(B)** Concentration (µmol L^{-1}) of soil media and cultures at steady state. NO_3^- and NO_2 are subtracted from DON, while ammonium is still included. Error bars represent the standard deviation.

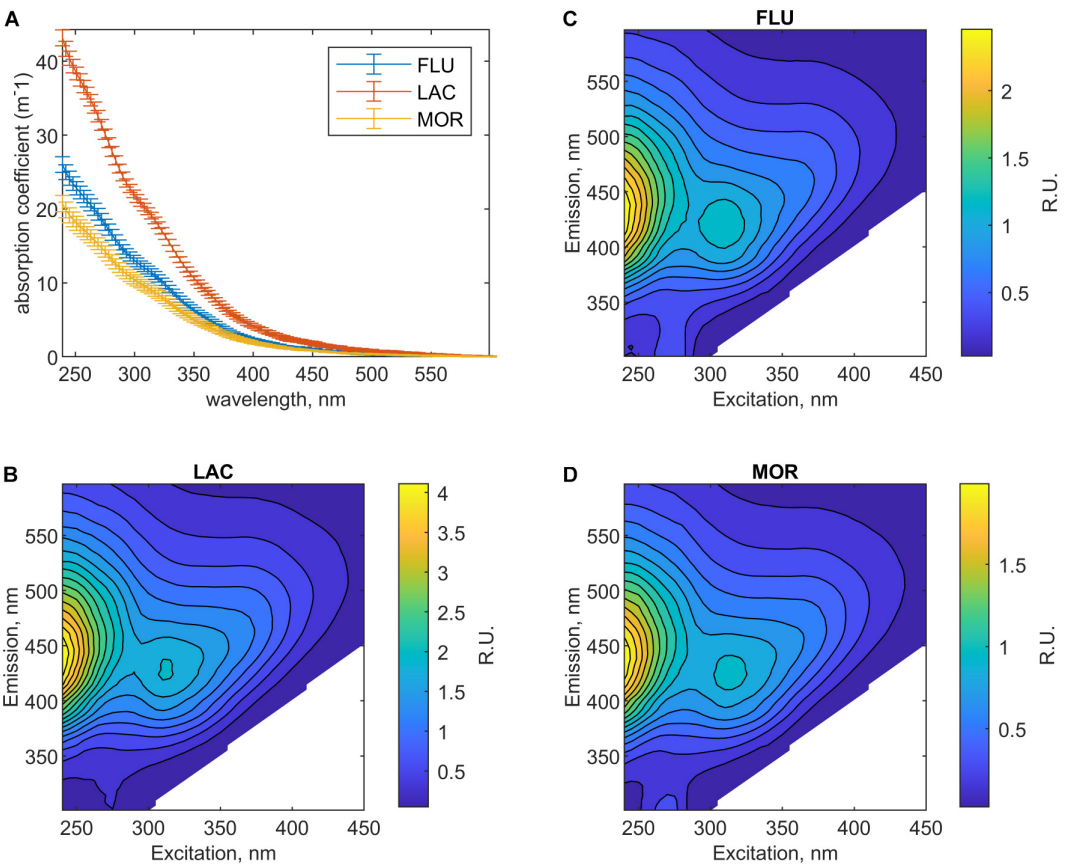

FIGURE 3 | Mean absorption spectra **(A)** and fluorescence EEMs (**B–D**, displayed as Raman units, R.U.) for the filtered media at steady-state. **(B)** LAC, **(C)** FLU, and **(D)** MOR.

TABLE 1 | Mean spectral slopes [*S*(275–295) and *S*(350–400)], slope ratios (S_r), $SUVA_{254}$ values (calculated from the soil medium CDOM spectra) and intensities of five commonly reported fluorescence peaks (Coble, 1996) (peak *A* = Ex/Em: 260/430, peak *B* = Ex/Em: 275/305, peak *C* = Ex/Em: 340/440, peak *M*: Ex/Em: 300/390, and peak *T* = Ex/Em: 275/340) for the three glacial deposit types.

DOM characteristics	Proxy	FLU	LAC	MOR
***S*(275–295) (μm^{-1})**	Molecular weight; photobleaching	**13.4** (±0.29)	**13.7** (±0.22)	**13.4** (±0.31)
***S*(350–400) (μm^{-1})**	Molecular weight; photobleaching	**21.3** (±0.69)	**19.2** (±0.59)	**19.6** (±0.70)
S_r	Molecular weight; origin of water	**0.63** (±0.02)	**0.71** (±0.02)	**0.68** (±0.00)
$SUVA_{254}$ (L mg C^{-1} m^{-1})	Aromaticity	**1.65** (±0.06)	**2.15** (±0.05)	**1.17** (±0.06)
Peak A (R.U.)	Humic-like compounds; terrestrial	**1.73** (±0.05)	**2.79** (±0.05)	**1.38** (±0.08)
Peak B (R.U.)	Tyrosine and protein-like compounds; autochthonous	**0.50** (±0.04)	**0.29** (±0.02)	**0.32** (±0.15)
Peak C (R.U.)	Humic-like compounds; terrestrial	**0.95** (±0.03)	**1.69** (±0.04)	**0.85** (±0.06)
Peak M (R.U.)	Marine humic-like compounds;	**1.07** (±0.04)	**1.42** (±0.03)	**0.76** (±0.05)
Peak T (R.U.)	Tryptophan and protein-like compounds; autochthonous	**0.40** (±0.03)	**0.39** (±0.01)	**0.24** (±0.03)

R.U. corresponds to Raman units. Numbers in bold represent mean values, while numbers in parentheses represent standard deviations.

TABLE 2 | Overview of the carbon processing at 24 h timescale due to microbial activity in the cultures.

Glacial deposit type	Respiration (μM O_2 d^{-1})	Bacterial carbon production (μM C d^{-1})	DOC uptake (μM C d^{-1})	BGE (%)
FLU	**90** (±12, *n* = 8)	**16** (±13, *n* = 26)	**132**(±50, *n* = 28)	**13**(±12, *n* = 25)
LAC	**57** (±20, *n* = 8)	**48** (±37, *n* = 26)	**160** (±46, *n* = 28)	**28**(±20, *n* = 23)
MOR	**111** (±17, *n* = 8)	**105** (±58, *n* = 28)	**158** (±48, *n* = 28)	**66**(±42, *n* = 26)

The numbers are calculated as the mean value over the whole steady state period. Numbers in bold represent mean values, while numbers in parentheses represent standard deviations. The standard deviation indicates the variation across all the samples measured from different days and replicates.

marine microbial communities in the cultures, with a negative change corresponding to degradation and a positive change to production of CDOM. For FLU, the absorption between 239 and 450 nm was significantly lower in the culture compared to the medium during the steady state period (*t*-test, $p < 0.05$). A similar yet weaker change was apparent for LAC and only significant at wavelengths between 308 and 371 nm (*t*-test, $p < 0.05$). The reduction in CDOM absorption at 330 nm, for FLU and LAC was respectively −1.32 (±0.28, $n = 23$) m^{-1} and −0.70 (±0.35, $n = 22$) m^{-1} and significantly different (ANOVA, $p < 0.01$). For MOR, there was a significant production in CDOM absorption between 239 and 296 nm (*t*-test, $p < 0.05$, $n = 24$) and no significant change at 330 nm (*t*-test, $p > 0.05$).

The fluorescence properties of DOM were altered by the marine microbial communities, but the extent to which the EEM area was altered differed in between all three glacial deposit types (**Figures 5A–C**). The change in fluorescence intensity between FLU medium and culture was significant for all peaks (*t*-test, $p < 0.05$) and the change in peak A, peak B, peak C, peak M, and peak T, corresponded, respectively, to −0.15 (±0.07, $n = 23$), −0.18 (±0.04, $n = 23$), −0.06 (±0.04, $n = 23$), −0.14 (±0.04, $n = 23$), and −0.05 (±0.05, $n = 23$) R.U. (**Figure 5A**). For LAC, the change in fluorescence intensity was only significant for peak B and peak M (*t*-test, $p < 0.05$) and corresponded, respectively, to 0.05 (±0.02, $n = 22$) and −0.07 (±0.04, $n = 22$) R.U. (**Figure 5B**). As seen from **Figures 5D,G**, both the spectral characteristics of the fluorescence loss in the peak A and M regions in the FLU and LAC deposit types was very similar, although the microbial community in FLU removed much more from the medium (**Table 1**). The spectral characteristics of the fluorescence change in peak B region was also similar between FLU and LAC cultures (**Figure 5E**), however, there was a large removal in the FLU culture, while there was a weak, but still significant production in the LAC culture. The fluorescence loss in the region of peak C was comparable in character and intensity of removal for both FLU and LAC cultures (**Figure 5F**), even though there were differing start concentrations in the respective media (**Table 1**). For MOR, we observed no significant removal of fluorescence but rather

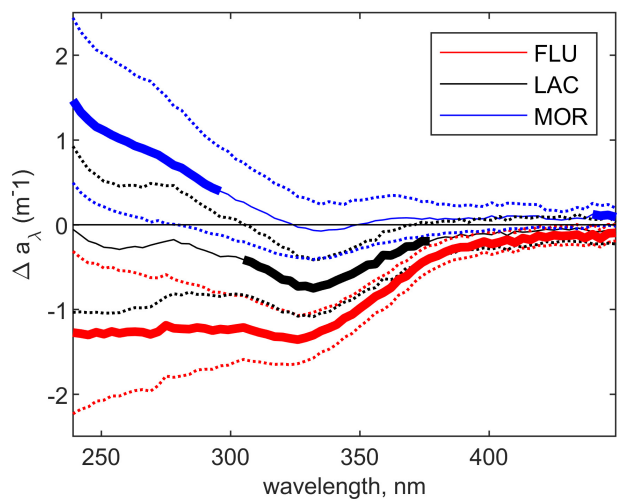

FIGURE 4 | Mean absorbance change between culture and medium at steady-state for each glacial deposit type. The dotted lines are displaying the standard deviation across all measurements in the steady-state period for each glacial deposit type ($n = 28$). The bold line is showing the area of the absorption spectrum that has significantly changed (*t*-test, $p < 0.05$).

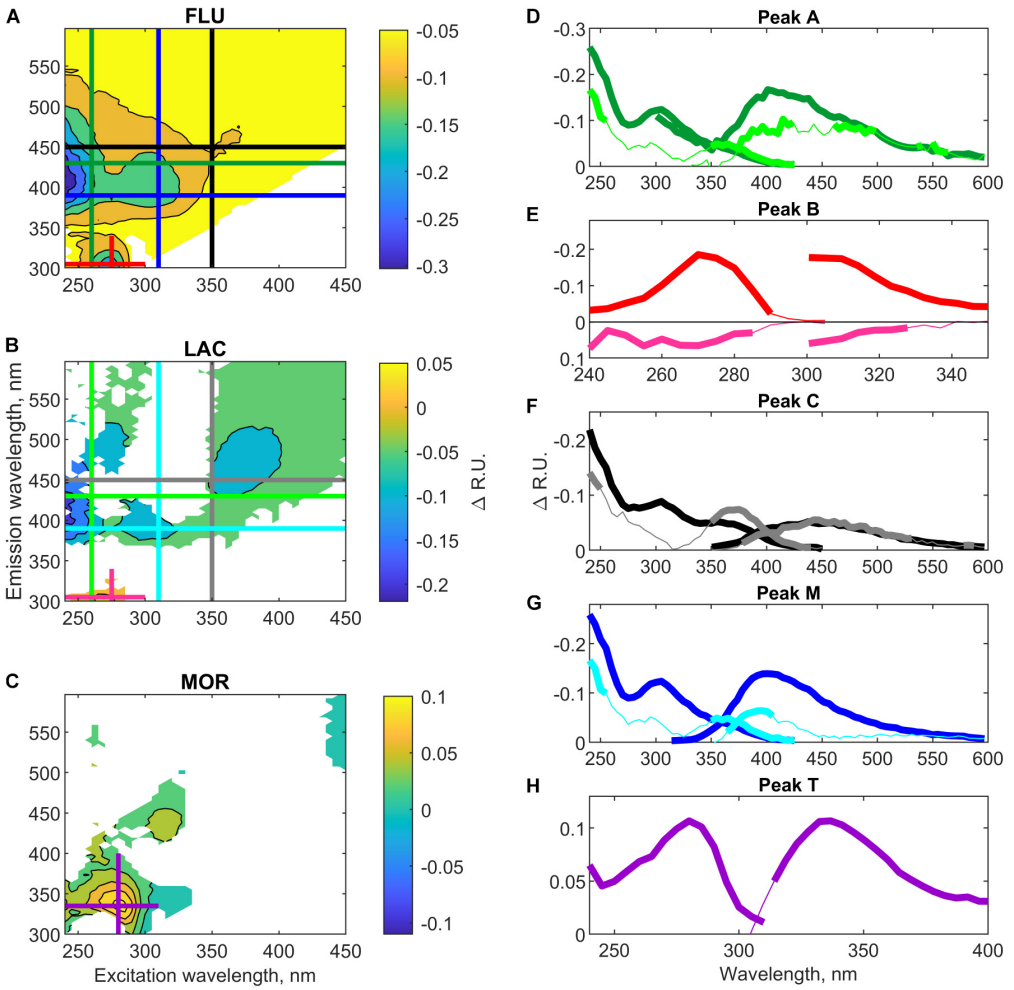

FIGURE 5 | Mean fluorescence change (Raman units, R.U.) between culture and medium at steady-state for each glacial deposit type. Panels **(A–C)** Shows the excitation-emission-matrix (EEM) with areas that are significant ($p < 0.05$) changed from the medium. **(A)** FLU, **(B)** LAC, and **(C)** MOR. Panels **(D–H)** Shows the excitation and emission spectra at specific emission and excitation wavelengths for different peaks. Panel **(D)** Peak A, **(E)** Peak B, **(F)** Peak C, **(G)** Peak M, and **(H)** peak T. The bold line shows which area is significant different from the soil medium. Note the *y*-axis changes, negative values represent a removal of fluorescence and positive values a production.

a significant production of peak T fluorescence by 0.10 (±0.03, $n = 24$) R.U. (**Figures 5C,H**).

Bacterial Growth and Bacterial Community Composition

At steady state the average BA was significantly different between all the three glacial deposit types (Kruskal–Wallis, $p < 0.005$) and the average abundance was 9.2 (±2.5, $n = 28$) 10^6 cell/mL in FLU culture, 32.1 (±14.6, $n = 28$) 10^6 cell/mL in LAC culture and 45.7 (±14.2, $n = 28$) 10^6 cell/mL in MOR culture.

Analysis of BCC was based on the % of reads. The BCC in the start cultures (**Figure 6A**) were dominated by *Gamma-* and *Alphaproteobacteria* in all cultures. In the FLU start culture, the bacterial community was composed of 48% *Gammaproteobacteria*, 42% *Alphaproteobacteria* and 10% *Bacteroidetes*. For LAC, the start culture had a BCC of 91% *Gammaproteobacteria*, 8% *Alphaproteobacteria* and 1% *Bacteriodetes*. Last, the MOR start culture had a BCC of 61% *Gammaproteobacteria*, 36% *Alphaproteobacteria*, and 3% *Bacteroidetes*. Other taxa contributed to less than 0.5% of the sequences in each of the three glacial deposit types. In the start cultures, the dominant order within *Alphaproteobacteria* was *Rhodobacterales* which contributed to 99, 87, and 98% of the *Alphaproteobacterial* reads in FLU, LAC, and MOR, respectively. In LAC start culture, the abundance of *Sphingomonadales* was 11% (**Supplementary Table 1**). Within *Gammaproteobacteria* the dominant orders in all treatments were *Oceanospirillales* and *Burkholderiales*. In the MOR start culture, *Cellvibrionales* and *Nitrosococcales* were also important and the abundance of each of these orders were 15% (**Supplementary Table 1**).

During the steady state period (**Figure 6B**), the bacterial community in the FLU and LAC cultures became dominated by *Alphaproteobacteria* [67% (±5, $n = 12$) and 87% (±13,

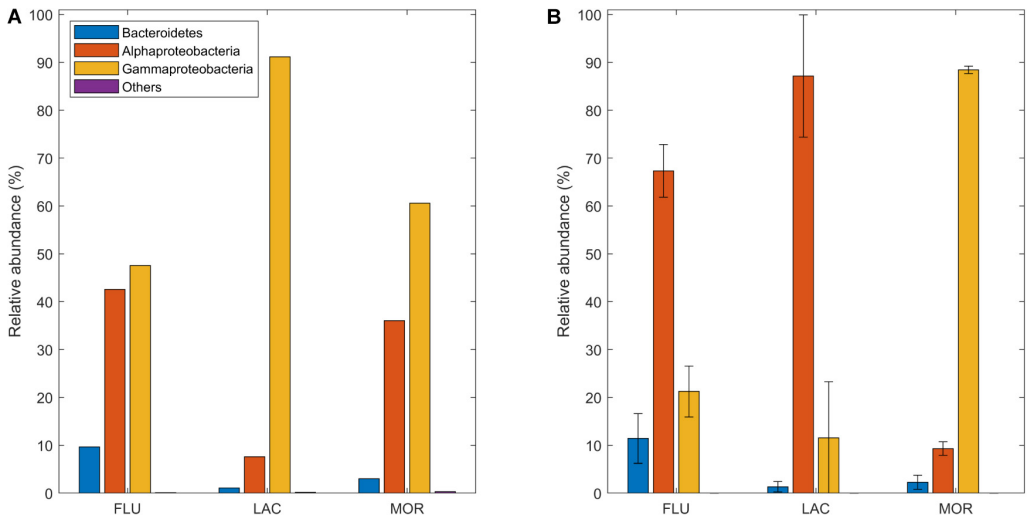

FIGURE 6 | Relative abundance of taxa (% of total number of reads) found in the culture for each glacial deposit type **(A)** Prior to the chemostat experiment and **(B)** During steady state of the chemostat experiment.

n = 12), for FLU and LAC, respectively]. In contrast the community in the MOR culture became more dominated by *Gammaproteobacteria* [88% (±1, n = 12)]. The abundance of other taxa remained very low in the cultures from all three glacial deposit types. At steady state, *Rhodobacterales* was the dominant order within *Alphaproteobacteria* within all glacial deposit types and contributed to between 79 and 98% of the Alphaproteobacterial reads. Other orders contributing to at least 1% of the reads in at least one of the glacial deposit types were *Sphingomonadales*, *Caulobacterales* and *Rhizobiales* (**Supplementary Table 1**). Within *Gammaproteobacteria*, *Oceanospirillales* was the dominant order in the cultures from all glacial deposit types and contributed to between 79 and 99% of the Gammaproteobacterial reads. In the FLU and LAC cultures the abundance of *Nitrosococcales* was 14% and 13% of the reads, respectively. Other orders with an abundance above 1% in at least one of the glacial deposit types were *Alteromonadales* and *Cellvibrionales* (**Supplementary Table 1**).

Based on tagwise dispersion analysis, 125 ASVs differed significantly in abundance between the MOR and the FLU cultures, 157 ASVs between the LAC and FLU cultures and 144 ASVs between the LAC and MOR cultures (**Supplementary Tables 2–4**). Based on the top 10 ASVs there was a significant higher abundance of ASVs belonging to the genus *Sulfitobacter* in the FLU cultures compared to both the LAC and MOR cultures (**Supplementary Tables 2**, **3**). In the LAC culture several of the ASVs with significantly higher abundance compared to the FLU and MOR cultures belonged to the genus *Pacificibacter* and *Polaribacter* (**Supplementary Tables 3**, **4**). Whereas in the MOR culture several of the ASVs belonged to the genus *Amphritea* and *Marinomonas* (**Supplementary Tables 2**, **4**).

During the development of all the cultures, bacterial community richness decreased, while community evenness either increased slightly (FLU and LAC) or decreased drastically (MOR) (**Supplementary Table 5**). During the steady state, both richness and evenness were significantly higher in FLU compared to both LAC and MOR (Kruskal–Wallis, $p < 0.05$).

During the steady state period the cultures from the different glacial deposit types formed three clearly distinct clusters (**Figure 7**) indicating that the composition of bacterial communities in cultures was significantly different between glacial deposit types (PERMANOVA, F = 36.75, $r2$ = 0.67, $p < 0.01$), despite starting with the same marine inoculum. Replicates from the same glacial deposit type were very similar indicating good reproducibility in the BCC. For MOR and LAC cultures, there was a clear development from the start community to the steady state community, whereas for the FLU culture the start and steady state communities were rather similar. Significant DOM characteristics plotted as vectors on the NMDS plot indicate that BCC is linked to DOM composition of the medium (**Figure 7B** and **Supplementary Table 6**) and that the different glacial deposit types were linked to different DOM characteristics. The strongest predictors are peak A and peak C (R^2 0.9521, respectively, 0.9503). The BCC in the LAC culture was positively correlated to peak A and peak C but also to peak M and $SUVA_{254}$. The BCC in the FLU culture was positively correlated to peak B and negatively correlated to DOC concentration and S_r. In contrast, the BCC in the MOR culture was not positively correlated to any of the included DOM characteristics but negatively correlated to peak T. Bacterial community composition was also correlated to DOM utilization. Differences in BCC was significant correlated to BCP, BGE, ΔpeakA, ΔpeakB, ΔpeakC, ΔpeakM, and ΔpeakT (where Δ refer to the change between medium and culture, Mantel test, $p < 0.05$, Pearson r = 11–46%, n = 36, **Supplementary Table 7**).

Carbon Processing

Average respiration rates were calculated for two time periods, <12 and >12 h, as there was a significant (ANOVA, $p < 0.01$) decrease in rates for FLU and LAC (**Figure 8**). Initial respiration

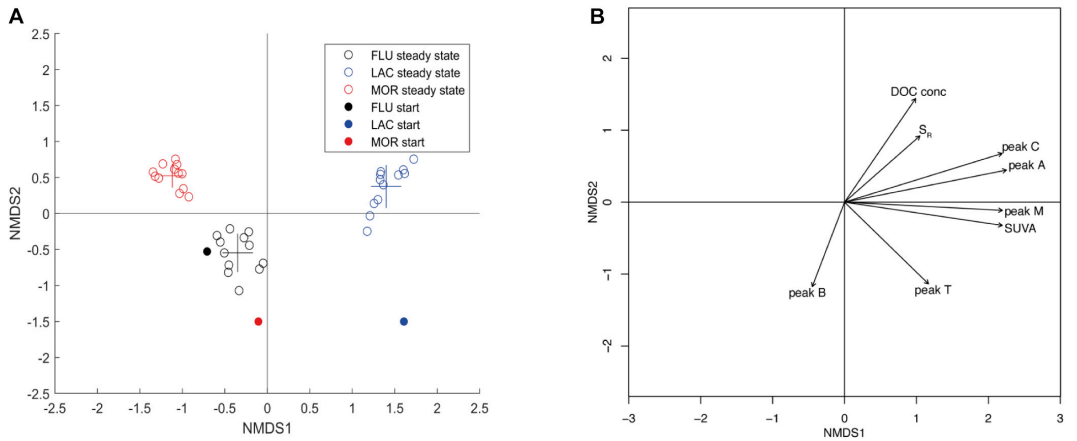

FIGURE 7 | (A) NMDS coordination plot based on 16S rRNA gene amplicon sequencing showing differences in bacterial community composition over time and between deposit types (Stress = 0.0903). Analysis is based on data from Illumina sequencing and Bray–Curtis dissimilarities. Glacial deposit type is indicated by color and time by filled and open circles (start and steady state). The center of the crosses represent the average (at steady-state) NMDS value of each glacial deposit type, while the length of the crosses represent the standard deviation. **(B)** NMDS coordination (as in **A**) with vectors indicating significant DOM characteristics of the medium. The direction of the vector indicate an increase of the variable and the length of the vector indicate the strength of the association.

rates were highest in FLU. For the second period (>12 h) FLU and LAC had comparable lower respiration rates while MOR maintained a respiration rate which was comparable to the initial stage (<12) (ANOVA, $p > 0.05$).

Bacterial carbon production rates were highest for the MOR culture, followed by the LAC and FLU cultures (**Table 2**) and the BCP rates differed significantly between all the glacial deposit types (Kruskal–Wallis, $p < 0.001$). Based on the change in DOC concentration (see section "Alteration of DOM in the Cultures") between medium and culture, the DOC uptake over 24 h (**Table 2**) was found to be similar between LAC and MOR, but significantly lower in FLU (ANOVA, $p < 0.01$, respectively). Bacterial growth efficiency (**Table 2**) was found to be significantly higher in the MOR culture (ANOVA, $p < 0.001$), while the BGE in the FLU and LAC cultures did not differ significant between each other (ANOVA, $p = 0.14$).

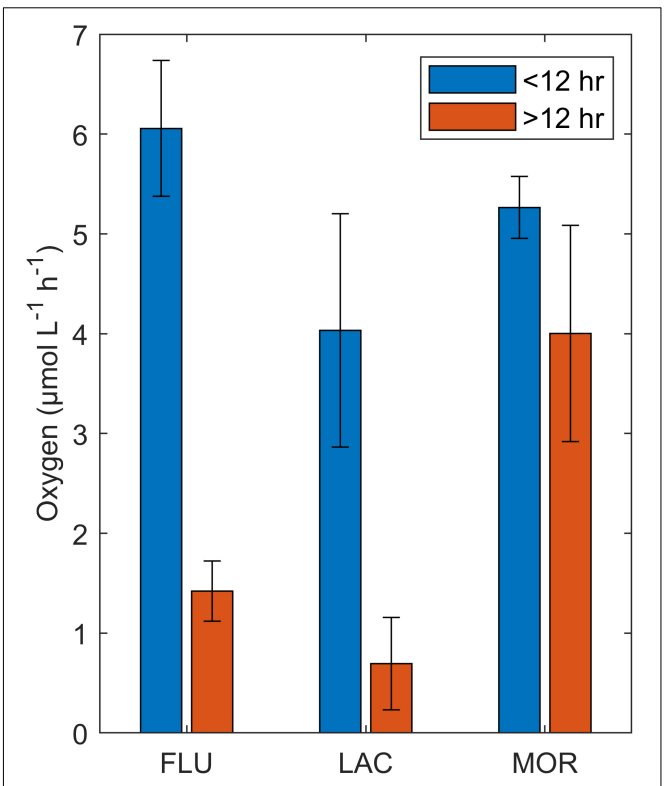

FIGURE 8 | Respiration rates (oxygen µmol L^{-1} h^{-1}) for each glacial deposit type, divided into two different categories <12 h (blue bar) and >12 h (red bar). Error bars represent standard deviation.

DISCUSSION

Characteristics of DOM in Media

Our results show that the composition and biodegradability of DOM differs between post-glacial landscape units and that these differences are related to the glacial processes. In agreement with our results, a recent study also found a coupling between permafrost soil formation and DOM character for different permafrost end-member types (tills, diamicton, lacustrine, peat, and Yedoma deposits) (MacDonald et al., 2021). In addition, different soil-forming factors such as ice content, permafrost extent and parent material (epigenetic vs. syngenetic formation) shape the biogeochemical response to permafrost thaw in aquatic systems (Tank et al., 2020). Factors such as grain size and the amount of minerals can also influence the OM content (Palmtag and Kuhry, 2018; Opfergelt, 2020). These findings underline that soil formation and erosion conditions play an important role when looking at DOM release due to coastal erosion, but at the same time highlight the complexity of studying biodegradation related to permafrost thaw. The differences in soil formation history, OC content, and grain size therefore likely

help explain some of the subtle differences we observed in DOM characteristics between our glacial deposit types.

The DOC:DON ratios (17–25) of the DOM in the media in this experiment indicate a high bioavailability of freshly eroded coastal permafrost soil. Ratios were on the whole lower than those for Arctic rivers [>50, (Dittmar and Kattner, 2003; Holmes et al., 2012)] but comparable to four different Arctic lagoons and coastal waters (16–19) near our sampling site (Dunton and Crump, 2014) as well as thermokarst feature outflows (19.5) (Abbott et al., 2014). Similarly to these studies, Dittmar and Kattner has reported an average DOC:DON ratio for the ACZ around the Laptev Sea of 21.4 (150 μM DOC and 7 μM DON). $SUVA_{254}$ is correlated to the aromatic content of DOM (Weishaar et al., 2003) and $SUVA_{254}$ from permafrost-derived DOM are expected to vary between 0.6 and 4.5 L mg C^{-1} m^{-1} (Ward and Cory, 2015; Raudina et al., 2017; Wickland et al., 2018; Coch et al., 2019; Fouché et al., 2020) depending on the OM content, with mineral soil types posing lower $SUVA_{254}$ values than organic soil types. In our study, the average $SUVA_{254}$ value across the three glacial deposit types was found to be 1.66 L mg C^{-1} m^{-1} and therefore fits with the reported average of 1.82 L mg C^{-1} m^{-1} obtained from 221 Arctic Canadian soil samples including active layer and permafrost layer (Fouché et al., 2020). Since the contribution of polyphenolic and condensed aromatic compounds leads to lower degradability of organic matter (Textor et al., 2019), we could therefore expect a higher bioavailability in MOR compared to FLU and LAC, based on the $SUVA_{254}$ values. As with the DOC:DON ratios, the $SUVA_{254}$ values are lower than that reported for DOM in Arctic rivers (Walker et al., 2013; Mann et al., 2016; O'Donnell et al., 2016; Coch et al., 2019). DOM is transformed during the transport along the river (Drake et al., 2018; Zhang et al., 2020) and according to the River Continuum Concept it can be expected that labile DOM from the catchment would be rapidly removed, while more recalcitrant DOM would be transported downstream (Vannote et al., 1980). This might explain the higher $SUVA_{254}$ and DOC:DON ratio in Arctic rivers compared to the media used in the experiment.

Slope ratio has shown to be inversely correlated to molecular weight, with low values (<1.0) typical for terrestrial DOM (Helms et al., 2008). DOM extracted from Canadian Arctic soil types expect to have S_r values that range between 0.58 and 3.24 (Fouché et al., 2020). Ward and Cory (2015) demonstrated that the CDOM in the active layer and permafrost layer from soils in Alaska had S_r values of 0.72 and 0.96, respectively, while Wickland et al. (2018) reported S_r values ranging between 0.73 and 1.13 across the active layer and permafrost layer for three other soil types in Alaska (Orthels, Histels, and Turbels). S_r values increase as DOM is processed in natural settings, particularly via photodegradation (Helms et al., 2008). However, since our media has been kept in dark during the whole experiment, the S_r values in this study relate to the composition of CDOM rather than processing. In addition, it has been shown that lower spectral slopes in the UVA area for Arctic coastal water is not correlated with photodegradation (Juhls et al., 2019), and that the lower spectral slope for UVA instead likely reflects lability of DOM (Matsuoka et al., 2015). Therefore, we conclude that the significant differences in S_r values between the three glacial deposit types underline differences in the DOM composition. The higher UVA spectral slope for FLU medium compared to LAC and MOR media (**Table 1**) indicates a lower bioavailability of the DOM pool in this glacial deposit type and fits with results from the BGE values (**Table 2**).

An important difference between the DOM from natural coastal erosion and the DOM in this experiment is the fact that the media was autoclaved. Autoclaving might cause changes in DOM composition due to hydrolysis and denaturation of various compounds and colloids (Dill and Shortle, 1991; Druart and De Wulf, 1993) and, therefore, also changes in bioavailability. However, all the parameters reported above were within natural ranges for soils found in the study region. In addition, it has been shown that even if autoclaving changed DOC in an unpredictable manner, it did not cause a convergence of the DOC pool from different lakes (Andersson et al., 2018). This means that although DOC is not identical to the initial conditions after autoclaving, the diversity of DOC is preserved.

Optical Signature of Microbial Degradation

The microbial degradation of the DOM in the media imparted an optical signature on the absorption and fluorescence properties of the DOM. Despite the fact that the initial spectral characteristics of the DOM in the media were only subtly different between glacial deposit types, the results show significant differences in DOM turnover. The high utilization rate of permafrost-derived DOM has been correlated to the relative high abundance of hydrogen-rich compounds, such as aliphatic molecules (amino acids, peptides, and protein) and carbohydrates (Spencer et al., 2015; Stapel et al., 2017; Textor et al., 2018, 2019). Lower degradability of organic matter in some soils has on the other hand been correlated with a greater contribution of polyphenolic and condensed aromatic compounds, often linked to decomposition processes of the overlying vegetation during unfrozen periods (Textor et al., 2019). Although harder for bacteria to utilize, compounds such as lignin phenols and related poly-phenolic compounds, can be metabolized or transformed into other compounds (Fasching et al., 2014).

Even though the highest amount of DOC was degraded in the MOR culture (**Figure 2**), the optical signature indicated a net production of CDOM and FDOM (**Figures 4**, **5**). Production of fluorescence peaks B and T in coastal waters are known to be correlated to amino acids produced by bacterial communities (Yamashita and Tanoue, 2003). This production of CDOM and FDOM, together with the high DOC removal, suggests that the DOM derived from the MOR deposit type contains a high amount of colorless labile DOM compounds (less conjugated aliphatic molecules). Since these compounds are easier for bacteria to utilize (Berggren et al., 2010), CDOM and FDOM would not be degraded as long as these labile DOM compounds are available. The high amount of colorless DOM can probably be explained by the glacial formation process behind MOR. Since the MOR deposit type was not submerged in water during glacial processes (Krzic et al., 2010), little prior decomposition of these

less conjugated aliphatic compounds has occurred. The upper permafrost layer of MOR may have thawed during the Holocene Thermal Maximum, where active layer depths reached more than 1 m (Burn, 1997), which could have resulted in intensive carbon degradation under aerobic conditions as a topographic gradient remained. However, this assumption remains speculative for our sampled sites.

From the optical signature (**Figures 4**, **5**), the FLU culture showed degradation of CDOM and FDOM compounds across the whole absorbance spectrum and fluorescence EEM. This suggests that only a very small amount of colorless bioavailable DOM was present and that the microbial community degraded the bioavailable CDOM and FDOM, such as labile conjugated aliphatic and aromatic compounds, immediately. This assumption fits well with the FLU deposit type, which potentially lacks less conjugated and colorless labile aliphatic compounds, previously leached from vegetation into the active layer (Textor et al., 2019). The lack of these compounds could be due to degradation when the FLU deposit type was submerged under stagnant waters during glacial processes in the Holocene Thermal Maximum (Krzic et al., 2010; Schirrmeister et al., 2011), thereby leaving a higher abundance of more conjugated aliphatic and aromatic compounds behind when the soil permanently refroze after this period.

For the LAC culture, we observed a production of peak B (**Figure 5**), which could indicate that the DOM derived from the LAC deposit type was transformed into FDOM compounds upon microbial degradation (Yamashita and Tanoue, 2003; Fasching et al., 2014). However, in contrast to the MOR culture, the LAC culture also degrades CDOM and FDOM compounds (**Figures 4**, **5**), such as labile conjugated aliphatic and aromatic compounds, probably as the competition for the colorless labile DOM increases. Similar to the FLU deposit type, the LAC deposit type was also submerged in water during glacial processes (Krzic et al., 2010), resulting in the degradation of less conjugated and colorless aliphatic compounds prior to our sampling (Walter Anthony et al., 2018). In contrast to the fluvial environment, the lacustrine environment has probably allowed a production of colorless aliphatic compounds (Meyers and Ishiwatari, 1995; Schirrmeister et al., 2011), such as OM excreted from phytoplankton and heterotrophic species which can be very labile compounds and often support bacterial growth (Rosenstock and Simon, 2001; Kinsey et al., 2018).

Our results suggest that the DOM composition in Cryosols with a different glacial geomorphic history, induce marine microbial communities to impart different optical degradation signatures, ultimately indicating differences in biodegradability among the glacial deposit types. The results also indicate that DOM in the media is more bioavailable than riverine terrestrial DOM, since several studies found no to very low degradation by marine microbial communities as the riverine terrestrial DOM enters coastal waters (Köhler et al., 2003; Amon and Meon, 2004; Herlemann et al., 2014; Blanchet et al., 2017). Large rivers have already lost most of the labile ancient soil DOM components at the time the material reach the ACZ, as degradation occurs mostly in uplands and headwaters (Drake et al., 2015; Spencer et al., 2015). Nonetheless, it can therefore be argued that DOM released from coastal erosion of Cryosols will have a larger impact on the coastal environment in the ACZ than that of riverine DOM.

Substrate Driven Community Differences

The observed distinct patterns in BCC between the three glacial deposit types, used in this experiment, reflect the subtle underlying differences in DOM quality (**Figure 7** and **Supplementary Table 1**). The grouping of the BCC across replicates (**Figure 7**) within each soil treatment indicates a systematic DOM control on BCC development from a common marine inoculum community. Interestingly, the community composition in the MOR culture was not positively correlated to any of the DOM characteristics included in the analysis which might indicate that this community is selected by the colorless DOC dominating the MOR medium. This agrees with the negative correlation to peak T and $SUVA_{254}$ for MOR soil, which indicates a response to less degraded DOM pool with a lower aromaticity. In contrast, the BCC of FLU and LAC cultures were positively correlated to one or several of the DOM characteristics (**Table 1**). The positive correlation to peak B in the FLU medium indicate a response to a higher relative amount of protein-like compounds, whereas the positive correlation to peak A, peak C, peak M, and $SUVA_{254}$ in the LAC soil show a response to humic-like compounds (Coble, 2007; Stedmon and Nelson, 2015).

Common for all of the three different cultures was the reduction in species richness between start and steady state, which essentially indicates that cultivation in the chemostat selected bacterial communities that were best suited to the specific DOM derived from the glacial deposit types. The rise and dominance of *Gammaproteobacteria* and *Alphaproteobacteria* in these chemostat cultures agrees with results from regrowth batch experiments (Sipler et al., 2017; Müller et al., 2018). However, *Gammaproteobacteria* are commonly found to dominate biodegradation experiments, as these bacterial taxa are known to be opportunistic with high growth rate and ability to exploit available DOM (Herlemann et al., 2014). This was clearly the case for the MOR culture (**Figure 6**) where the highest DOC uptake and respiration rates were measured (**Figure 8**), coupled with CDOM and FDOM production (**Figures 4**, **5**). Combined these results indicate that moraine soil DOM contains colorless labile DOM which is rapidly degraded and supporting the development of the *Gammaproteobacteria* community. In the FLU and LAC cultures, we instead observed a dominance of *Alphaproteobacteria* (**Figure 6**). This difference in BCC was paralleled with the notable difference in CDOM and FDOM signatures imparted by the communities (Mantel tests, **Supplementary Table 3**). In FLU and LAC cultures, there were a significant removal of CDOM and FDOM (**Figures 4**, **5**). Although both dominated by *Alphaproteobacteria*, the FLU and LAC communities were also distinct (**Figure 7**) and this apparently influenced the extent of CDOM and FDOM removal (**Figures 4**, **5**).

Alphaproteobacterial reads were dominated by the order *Rhodobacterales* in cultures from all glacial deposit types, whereas *Oceanospirillales* was the dominant order among Gammaproteobacterial reads. However, the difference in BCC

was verified at the genus level where several ASVs differed significantly in abundance between the three glacial deposit types (tagwise dispersion analysis). There was significant higher abundance of ASVs belonging to the genus *Sulfitobacter* in the FLU culture, and members from this genus have been isolated from similar environments (Park et al., 2019). The first isolate and type specie, *Sulfitobacter pontiacus*, is a sulfur-oxidizing chemoheterotrophic bacteria which utilizes mainly carboxyl and amino acids (Sorokin, 1995). In the LAC cultures several of the ASVs with significantly higher abundance belonged to the genus *Polaribacter* and *Pacificibacter*. *Polaribacter* belongs to *Flavobacteria* (*Bacteroidetes*) which have been ascribed to act as degraders of high molecular weight OM, such as proteins and carbohydrates (Thomas et al., 2011). The type specie for *Pacificibacter*, *Pacificibacter maritimus*, was isolated from shallow marine sediments and utilizes mostly sugars, amino acids and a few carboxylic acids (Romanenko et al., 2011). And last, in the MOR culture several of the ASVs belonged to the genera *Amphritea* and *Marinomonas*. The majority of the members of the genus *Amphritea* are closely associated with living marine organisms, however, some members of the genus has been isolated from marine sediments (Miyazaki et al., 2008). Species within *Amphritea* oxidize various sugars and carboxylic acids (Gärtner et al., 2008). Members of the genus *Marinomonas* have a widespread distribution in marine environments and have for example been found in seawater (Yoon et al., 2005), sea ice (Zhang et al., 2008) and seafloor sediment (Romanenko et al., 2011). Based on the characterization of *Marinomonas polaris* and *Marinomonas arctica* the species utilize sugars, amino acids, and sugar alcohols, but not complex carboxylic acids and aromatic compounds (Gupta et al., 2006; Zhang et al., 2008).

Although it is hard to link these ASVs to specific characteristics of the DOM, these analyses show that the presence and abundance of specific phylotypes might determine the utilization of DOM. Our results are therefore in line with the growing number of studies linking community composition to OM lability (Cottrell and David, 2003; Gómez-Consarnau et al., 2012; Nelson and Carlson, 2012; Logue et al., 2016; Balmonte et al., 2019) and shows that the bioavailability should be seen as an interaction between the chemical composition of DOM and the metabolic capacity of the microbial community (Nelson and Wear, 2014).

Microbial Carbon Processing

Climate change will intensify erosion of Arctic coasts (Günther et al., 2015; Hoque and Pollard, 2016; Obu et al., 2016; Couture et al., 2018; Jones et al., 2018) but the ultimate fate of this carbon source is still unknown (Fritz et al., 2017). Understanding how DOC from different glacial deposit types will be mobilized by bacteria in the ACZ could eventually help us quantify the fate of carbon export from eroding soils along Arctic coastlines. We acknowledge the important difference between natural coastal erosion and our experiment, where coastal erosion will add both OM and *in situ* microbial communities to the marine water. Recent studies along aquatic continua have shown that microbial communities in lakes and streams contain organisms with terrestrial origins (Crump et al., 2012; Ruiz-González et al., 2015; Hauptmann et al., 2016). However, it is not clear whether bacteria transported with soil will be active and thrive in sea water since salinity is one of the strongest environmental filters (Langenheder et al., 2003). In addition to 'species sorting' which probably will take place in response to this chemical limit (Van der Gucht et al., 2007) there will also be priority effects for well established communities (Svoboda et al., 2018). We therefore believe that most of the carbon reaching the ACZ due to coastal erosion will be processed by the marine bacterial community.

In this study we demonstrate that not only are colorless DOM compounds being mobilized by marine microbial communities when Cryosols are released into the ACZ, but also that CDOM and FDOM compounds are bioavailable to marine microbial communities. The DOC removal by marine microbial degradation is the sum of carbon used for bacterial production and carbon released through respiration (**Table 2**). The bacterial production achieved by the chemostat cultures is dependent on the dilution rate, the quality of substrate (DOM bioavailability) and the ability of the community to utilize the substrate (Del Giorgio and Cole, 1998). As the dilution rates were set constant, the differences observed here reflect a combination of community composition and DOM character. The FLU culture had the lowest removal of DOC (**Figure 2** and **Table 2**) and lowest BCP. MOR and LAC cultures achieved approximately 3–4 times higher BA than FLU and abundances were higher than those often achieved in bottle experiment (Sipler et al., 2017; Müller et al., 2018), where supply of substrate is limited. Although the DOC removal was similar between the MOR and LAC cultures, BCP was two times higher in the MOR cultures.

Differences in BCP will have consequences for bacterial growth efficiency (BGE) which is a measurement of how efficiently carbon is converted into biomass (Del Giorgio and Cole, 1998). BGE has been shown to be strongly correlated with the composition of terrestrial DOM (Berggren et al., 2007). BGE in our study varied between 13 and 66% with highest values in the MOR culture and lowest in the FLU culture. Estimates of BGE for natural aquatic bacterial communities range from 5 to 60% with the highest values usually found in coastal waters and estuaries (Del Giorgio and Cole, 1998). However, in the Arctic region other studies have found the BGE to be 19.5% within Arctic Rivers and between 7 and 10% within Arctic Fjords (Middelboe et al., 2012; Paulsen et al., 2017), while it has been found to be lower in Arctic Ocean with 6.3% in the Fram Strait (Kritzberg et al., 2010) and 2.2% in the Chucki Sea (Cota et al., 1996). The fact that the BGE results from our study exceeds what has been previously found within other aquatic ecosystems throughout the Arctic Ocean, therefore suggest that the DOC from freshly exposed Cryosols could be one of the most labile sources of carbon in this region. In addition, the high variation in BGE between glacial deposit types suggest that the lability of DOC depends heavily on the specific deposit type being eroded. The increased rate of coastal erosion and thereby release of highly bioavailable DOM can therefore have a huge impact on the marine microbial communities in the ACZ.

Several studies have shown that a potentially large amount of CO_2 is released during coastal erosion due to microbial processes (Vonk et al., 2012; Semiletov et al., 2013; Tanski et al., 2019). Our results on BCP and respiration show that carbon processing by the marine microbial communities will lead to different fates of the DOC depending on the glacial deposit type. With a lower BGE, lower amounts of bioavailable DOC are stored as biomass in the marine microbial communities and more of the carbon may be respired to the atmosphere as CO_2, as seen for the FLU deposit type. However, the majority of DOC was indeed refractory to biodegradation. This refractory DOC may be exported further out into ACZ where it may end up being buried in sediments or stored in the deep ocean.

Summary of Findings and Future Implications

Coastal erosion in the Arctic is intensifying and DOM from Cryosols will become an even more important source in the ACZ in the future. Here we show that the composition and biodegradability of DOM differs between post-glacial landscape units and that the differences in DOM composition and biodegradability are related to the glacial processes.

The three different DOM sources (FLU, LAC and MOR) supported the development of three different marine microbial communities, which was especially clear when comparing the MOR deposit type to FLU and LAC. These findings indicate a clear substrate-driven control on marine microbial community composition, especially where the input of organic carbon and DOM in the ACZ is dominated by release from coastal erosion of Cryosols. The bacterial communities imparted different spectral fingerprints on the absorption spectra and fluorescence EEMs of the DOM. Based on these fingerprints, we show that both colorless DOM and labile CDOM and FDOM fractions are being degraded. Also, the spectral results suggest that the more refractory CDOM and FDOM pool can be associated with CDOM and FDOM found in the open ocean after passing the ACZ. In addition, we show that absorbance at 330 nm could to be a proxy of microbial degradation of CDOM, especially produced in FLU and LAC deposit types during the Holocene Thermal Maximum.

The chemostat approach applied here provides a simulation of the constant substrate supply to coastal waters that can occur during summer open water conditions with maximum permafrost erosion rates. However, the results from this experiment will not fully represent what is happening in the natural environment. Important differences include the higher-than-natural incubation temperature at 20°C, which is standard for bioavailability studies, but might affect both the activity and composition of the bacterial community (Pomeroy and Wiebe, 2001; Adams et al., 2010; Sjöstedt et al., 2012a), together with autoclaving of the media, which can cause changes in the bioavailability and composition of the DOM. However, chemostats has been suggested to be the method that most closely resembles the growth conditions bacteria encounter in natural systems (Kovárová-Kovar and Egli, 1998) and the reproducibility between the replicate chemostats provide confidence in the robustness of this method. It is therefore clear that DOM quality influences the BCC, which in turn also affects the net effect of DOM degradation. Moraine deposit type will result in the net production of CDOM and FDOM in coastal waters, while the deposits types that are formed in aquatic environments, such as FLU and LAC, will lose CDOM and FDOM as it passes through coastal waters. These findings suggest a continuum, where the presence of ancient colorless labile DOM supports a rapidly growing community and a net production of CDOM and FDOM, which in turn can be degraded by other members of the bacterial communities with the capacity to degrade CDOM and FDOM.

To achieve a better understanding of carbon turnover from coastal erosion of Cryosols in the ACZ and its effects on climate and ecology in the future, more studies including qualitative measurements on DOM, such as absorbance and fluorescence spectroscopy, coupled with both bacterial and phytoplankton community assessment should be performed. Nevertheless, it is important to note that a large proportion of bioavailable DOM in these systems may not be captured and characterized using optical measurements.

DATA AVAILABILITY STATEMENT

The datasets generated for this study can be found online using the following link: https://doi.org/10.11583/DTU.14113250.v1. The names of accession number(s) can be found below: https://www.ncbi.nlm.nih.gov/, PRJNA675030.

AUTHOR CONTRIBUTIONS

AB, CS, and JS planned and performed the experiments. AM, NS, GT, and JV led sampling site selection and coordinated and performed field sampling. AB, CS, JS, and JC analyzed samples and performed data analysis. AB, CS, and JS wrote the manuscript. All authors commented on the manuscript and contributed to the interpretation and discussion of the results.

FUNDING

This publication is part of the Nunataryuk project. The project has received funding under the European Union's Horizon 2020 Research and Innovation Programme under grant agreement no. 773421. Part of this research was supported by Japan Aerospace Exploration Agency (JAXA) Global Change Observation Mission-Climate (GCOM-C) to AM (contract #20RT000350), Independent Research Fund Denmark (9040-00266B) awarded to CS, and by the Swedish Research Council (VR, grant 2015-00188) to JS, and the Natural Sciences and Engineering Research Council of Canada (Discovery program, RGPIN-2020-06874) to JC.

ACKNOWLEDGMENTS

We acknowledge colleagues in the EU Horizon 2020 Nunataryuk project (grant no. 773421) who contributed to the sampling and logistics and colleagues at Plateforme d'Analyses Génomiques (IBIS, Université Laval, Quebec City, Canada) for performing the Illumina sequencing. H. Lantuit, M. Fritz, and G. Hugelius are thanked for providing logistical and technical support. We also thank Lea Tolstrup for assistance during the chemostat experiment. Finally we thank the editor and the three reviewers for their valuable comments.

SUPPLEMENTARY MATERIAL

The Supplementary Material for this article can be found online at: https://www.frontiersin.org/articles/10.3389/feart.2021.640580/full#supplementary-material

REFERENCES

Abbott, B. W., Larouche, J. R., Jones, J. B., Bowden, W. B., and Balser, A. W. (2014). Elevated dissolved organic carbon biodegradability from thawing and collapsing permafrost. *J. Geophys. Res. Biogeosci.* 119, 2049–2063. doi: 10.1002/2014JG002678

Adams, H. E., Crump, B. C., and Kling, G. W. (2010). Temperature controls on aquatic bacterial production and community dynamics in arctic lakes and streams. *Environ. Microbiol.* 12, 1319–1333. doi: 10.1111/j.1462-2920.2010.02176.x

Amon, R. M. W., and Meon, B. (2004). The biogeochemistry of dissolved organic matter and nutrients in two large Arctic estuaries and potential implications for our understanding of the Arctic Ocean system. *Mar. Chem.* 92, 311–330. doi: 10.1016/j.marchem.2004.06.034

Andersson, M. G. I., Catalán, N., Rahman, Z., Tranvik, L. J., and Lindström, E. S. (2018). Effects of sterilization on dissolved organic carbon (DOC) composition and bacterial utilization of DOC from lakes. *Aquat. Microb. Ecol.* 82, 199–208. doi: 10.3354/ame01890

Arrigo, K. R., and Brown, C. W. (1996). Impact of chromophoric dissolved organic matter on UV inhibition of primary productivity in the sea. *Mar. Ecol. Prog. Ser.* 140, 207–216. doi: 10.3354/meps140207

Balmonte, J. P., Buckley, A., Hoarfrost, A., Ghobrial, S., Ziervogel, K., Teske, A., et al. (2019). Community structural differences shape microbial responses to high molecular weight organic matter. *Environ. Microbiol.* 21, 557–571. doi: 10.1111/1462-2920.14485

Belicka, L. L., Macdonald, R. W., and Harvey, H. R. (2002). Sources and transport of organic carbon to shelf, slope, and basin surface sediments of the Arctic Ocean. *Deep Sea Res. Part I Oceanogr. Res. Pap.* 49, 1463–1483. doi: 10.1016/S0967-0637(02)00031-6

Berggren, M., Laudon, H., Haei, M., Ström, L., and Jansson, M. (2010). Efficient aquatic bacterial metabolism of dissolved low-molecular-weight compounds from terrestrial sources. *ISME J.* 4, 408–416. doi: 10.1038/ismej.2009.120

Berggren, M., Laudon, H., and Jansson, M. (2007). Landscape regulation of bacterial growth efficiency in boreal freshwaters. *Glob. Biogeochem. Cycles* 21:GB4002. doi: 10.1029/2006GB002844

Biskaborn, B. K., Smith, S. L., Noetzli, J., Matthes, H., Vieira, G., Streletskiy, D. A., et al. (2019). Permafrost is warming at a global scale. *Nat. Commun.* 10:264. doi: 10.1038/s41467-018-08240-4

Blanchet, M., Pringault, O., Panagiotopoulos, C., Lefèvre, D., Charrière, B., Ghiglione, J.-F., et al. (2017). When riverine dissolved organic matter (DOM) meets labile DOM in coastal waters: changes in bacterial community activity and composition. *Aquat. Sci.* 79, 27–43. doi: 10.1007/s00027-016-0477-0

Burn, C. R. (1997). Cryostratigraphy, paleogeography, and climate change during the early Holocene warm interval, western Arctic coast, Canada. *Can. J. Earth Sci.* 34, 912–925. doi: 10.1139/e17-076

Callahan, B. J., McMurdie, P. J., Rosen, M. J., Han, A. W., Johnson, A. J. A., and Holmes, S. P. (2016). DADA2: high-resolution sample inference from Illumina amplicon data. *Nat. Methods* 13, 581–583. doi: 10.1038/nmeth.3869

Canelhas, M. R., Eiler, A., and Bertilsson, S. (2016). Are freshwater bacterioplankton indifferent to variable types of amino acid substrates? *FEMS Microbiol. Ecol.* 92:fiw005. doi: 10.1093/femsec/fiw005

Cauwet, G. (1999). ""Determination of dissolved organic carbon and nitrogen by high temperature combustion," in *Methods of Seawater Analysis*, eds K. Grasshoff, K. Kremling, and M. Ehrhardt (Weinheim: Wiley-VCH Verlag GmbH), 407–420. doi: 10.1002/9783527613984.ch15

Coble, P. G. (1996). Characterization of marine and terrestrial DOM in seawater using excitation-emission matrix spectroscopy. *Mar. Chem.* 51, 325–346. doi: 10.1016/0304-4203(95)00062-3

Coble, P. G. (2007). Marine optical biogeochemistry: the chemistry of ocean color. *Chem. Rev.* 107, 402–418. doi: 10.1021/cr050350

Coch, C., Juhls, B., Lamoureux, S. F., Lafreniére, M. J., Fritz, M., Heim, B., et al. (2019). Comparisons of dissolved organic matter and its optical characteristics in small low and high Arctic catchments. *Biogeosciences* 16, 4535–4553. doi: 10.5194/bg-16-4535-2019

Colatriano, D., Tran, P. Q., Guéguen, C., Williams, W. J., Lovejoy, C., and Walsh, D. A. (2018). Genomic evidence for the degradation of terrestrial organic matter by pelagic Arctic Ocean Chloroflexi bacteria. *Commun. Biol.* 1:90. doi: 10.1038/s42003-018-0086-7

Cota, G. F., Pomeroy, L. R., Harrison, W. G., Jones, E. P., Peters, F., Sheldon, W. M., et al. (1996). Nutrients, primary production and microbial heterotrophy in the southeastern Chukchi Sea:Arctic summer nutrient depletion and heterotrophy. *Mar. Ecol. Prog. Ser.* 135, 247–258. doi: 10.3354/meps135247

Cottrell, M. T., and David, K. L. (2003). Contribution of major bacterial groups to bacterial biomass production (thymidine and leucine incorporation) in the Delaware estuary. *Limnol. Oceanogr.* 48, 168–178. doi: 10.4319/lo.2003.48.1.0168

Couture, N. J., Irrgang, A., Pollard, W., Lantuit, H., and Fritz, M. (2018). Coastal erosion of permafrost soils along the yukon coastal plain and fluxes of organic carbon to the canadian beaufort sea. *J. Geophys. Res. Biogeosci.* 123, 406–422. doi: 10.1002/2017JG004166

Crump, B. C., Amaral-Zettler, L. A., and Kling, G. W. (2012). Microbial diversity in arctic freshwaters is structured by inoculation of microbes from soils. *ISME J.* 6, 1629–1639. doi: 10.1038/ismej.2012.9

Del Giorgio, P. A., and Cole, J. J. (1998). Bacterial growth efficiency in natural aquatic systems. *Annu. Rev. Ecol. Syst.* 29, 503–541. doi: 10.1146/annurev.ecolsys.29.1.503

Dill, K. A., and Shortle, D. (1991). Denatured states of proteins. *Annu. Rev. Biochem.* 60, 795–825. doi: 10.1146/annurev.bi.60.070191.004051

Dittmar, T., and Kattner, G. (2003). The biogeochemistry of the river and shelf ecosystem of the Arctic ocean: a review. *Mar. Chem.* 83, 103–120. doi: 10.1016/S0304-4203(03)00105-1

Dou, F., Ping, C.-L., Guo, L., and Jorgenson, T. (2008). Estimating the impact of seawater on the production of soil water-extractable organic carbon during coastal erosion. *J. Environ. Qual.* 37, 2368–2374. doi: 10.2134/jeq2007.0403

Drake, T. W., Guillemette, F., Hemingway, J. D., Chanton, J. P., Podgorski, D. C., Zimov, N. S., et al. (2018). The ephemeral signature of permafrost carbon in an arctic fluvial network. *J. Geophys. Res. Biogeosci.* 123, 1475–1485. doi: 10.1029/2017JG004311

Drake, T. W., Wickland, K. P., Spencer, R. G. M., McKnight, D. M., and Striegl, R. G. (2015). Ancient low-molecular-weight organic acids in permafrost fuel rapid carbon dioxide production upon thaw. *Proc. Natl. Acad. Sci. U.S.A.* 112, 13946–13951. doi: 10.1073/pnas.1511705112

Druart, P., and De Wulf, O. (1993). Activated charcoal catalyses sucrose hydrolysis during autoclaving. *Plant Cell Tiss. Organ Cult.* 32, 97–99. doi: 10.1007/BF00040122

Dunton, K., and Crump, B. (2014). *Collaborative Research: Terrestrial Linkages to Microbial and Metazoan Communities in Coastal Ecosystems of the Beaufort Sea*. Santa Barbara, CA: Arctic Data Center.

Environment Canada (2016). *Canadian Climate Normals*. Available online at: https://climate.weather.gc.ca/climate_normals/ (accessed February 1, 2021).

Fasching, C., Behounek, B., Singer, G. A., and Battin, T. J. (2014). Microbial degradation of terrigenous dissolved organic matter and potential consequences for carbon cycling in brown-water streams. *Sci. Rep.* 4:4981. doi: 10.1038/srep04981

Fouché, J., Christiansen, C. T., Lafrenière, M. J., Grogan, P., and Lamoureux, S. F. (2020). Canadian permafrost stores large pools of ammonium and optically distinct dissolved organic matter. *Nat. Commun.* 11:4500. doi: 10.1038/s41467-020-18331-w

Fritz, M., Opel, T., Tanski, G., Herzschuh, U., Meyer, H., Eulenburg, A., et al. (2015). Dissolved organic carbon (DOC) in Arctic ground ice. *Cryosphere* 9, 737–752. doi: 10.5194/tc-9-737-2015

Fritz, M., Vonk, J. E., and Lantuit, H. (2017). Collapsing arctic coastlines. *Nat. Clim. Chang.* 7, 6–7. doi: 10.1038/nclimate3188

Fritz, M., Wetterich, S., Schirrmeister, L., Meyer, H., Lantuit, H., Preusser, F., et al. (2012). Eastern Beringia and beyond: late Wisconsinan and holocene landscape dynamics along the Yukon Coastal Plain, Canada. *Palaeogeogr. Palaeoclimatol. Palaeoecol.* 319–320, 28–45. doi: 10.1016/j.palaeo.2011.12.015

Gärtner, A., Wiese, J., and Imhoff, J. F. (2008). *Amphritea atlantica* gen. nov., sp. nov., a gammaproteobacterium from the Logatchev hydrothermal vent field. *Int. J. Syst. Evol. Microbiol.* 58, 34–39. doi: 10.1099/ijs.0.65234-0

Gasol, J. M., and Del Giorgio, P. A. (2000). Using flow cytometry for counting natural planktonic bacteria and understanding the structure of planktonic bacterial communities. *Sci. Mar.* 64, 197–224. doi: 10.3989/scimar.2000.64n2197

Gómez-Consarnau, L., Lindh, M. V., Gasol, J. M., and Pinhassi, J. (2012). Structuring of bacterioplankton communities by specific dissolved organic carbon compounds. *Environ. Microbiol.* 14, 2361–2378. doi: 10.1111/j.1462-2920.2012.02804.x

Günther, F., Overduin, P. P., Yakshina, I. A., Opel, T., Baranskaya, A. V., and Grigoriev, M. N. (2015). Observing Muostakh disappear: permafrost thaw subsidence and erosion of a ground-ice-rich island in response to arctic summer warming and sea ice reduction. *Cryosphere* 9, 151–178. doi: 10.5194/tc-9-151-2015

Guo, L., and Macdonald, R. W. (2006). Source and transport of terrigenous organic matter in the upper Yukon River: evidence from isotope (δ^{13} C, Δ^{14} C, and δ^{15} N) composition of dissolved, colloidal, and particulate phases. *Glob. Biogeochem. Cycles* 20:GB2011. doi: 10.1029/2005GB002593

Gupta, P., Chaturvedi, P., Pradhan, S., Delille, D., and Shivaji, S. (2006). *Marinomonas polaris* sp. nov., a psychrohalotolerant strain isolated from coastal sea water off the subantarctic Kerguelen islands. *Int. J. Syst. Evol. Microbiol.* 56, 361–364. doi: 10.1099/ijs.0.63921-0

Hagstrom, Å, Ammerman, J. W., Heinrichs, S., and Azam, F. (1984). Bacterioplankton growth in seawater: II. Growth kinetics and cellular characteristicsin seawater cultures. *Mar. Ecol. Prog. Ser.* 18, 41–48.

Hansen, H. P., and Koroleff, F. (1999). "Determination of nutrients," in *Methods of Seawater Analysis*, eds K. Grasshoff, K. Kremling, and M. Ehrhardt (Weinheim: Wiley-VCH Verlag GmbH), 159–228. doi: 10.1002/9783527613984.ch10

Hauptmann, A. L., Markussen, T. N., Stibal, M., Olsen, N. S., Elberling, B., Baelum, J., et al. (2016). Upstream Freshwater and Terrestrial Sources Are Differentially Reflected in the Bacterial Community Structure along a Small Arctic River and its estuary. *Front. Microbiol.* 7:1474. doi: 10.3389/fmicb.2016.01474

Helms, J. R., Stubbins, A., Ritchie, J. D., Minor, E. C., Kieber, D. J., and Mopper, K. (2008). Absorption spectral slopes and slope ratios as indicators of molecular weight, source, and photobleaching of chromophoric dissolved organic matter. *Limnol. Oceanogr.* 53, 955–969. doi: 10.4319/lo.2008.53.3.0955

Herlemann, D. P., Labrenz, M., Jürgens, K., Bertilsson, S., Waniek, J. J., and Andersson, A. F. (2011). Transitions in bacterial communities along the 2000 km salinity gradient of the Baltic Sea. *ISME J.* 5, 1571–1579. doi: 10.1038/ismej.2011.41

Herlemann, D. P. R., Manecki, M., Meeske, C., Pollehne, F., Labrenz, M., Schulz-Bull, D., et al. (2014). Uncoupling of bacterial and terrigenous dissolved organic matter dynamics in decomposition experiments. *PLoS One* 9:e93945. doi: 10.1371/journal.pone.0093945

Heslop, J. K., Winkel, M., Walter Anthony, K. M., Spencer, R. G. M., Podgorski, D. C., Zito, P., et al. (2019). Increasing organic carbon biolability with depth in yedoma permafrost: ramifications for future climate change. *J. Geophys. Res. Biogeosci.* 124, 2021–2038. doi: 10.1029/2018JG004712

Holmes, R. M., McClelland, J. W., Peterson, B. J., Tank, S. E., Bulygina, E., Eglinton, T. I., et al. (2012). Seasonal and Annual Fluxes of Nutrients and Organic Matter from large rivers to the Arctic Ocean and surrounding Seas. *Estuar. Coasts* 35, 369–382. doi: 10.1007/s12237-011-9386-6

Hoque, M. A., and Pollard, W. H. (2016). Stability of permafrost dominated coastal cliffs in the Arctic. *Polar Sci.* 10, 79–88. doi: 10.1016/j.polar.2015.10.004

Hugelius, G., Strauss, J., Zubrzycki, S., Harden, J. W., Schuur, E. A. G., Ping, C. L., et al. (2014). Estimated stocks of circumpolar permafrost carbon with quantified' ' uncertainty ranges and identified data gaps. *Biogeosciences* 11, 6573–6593. doi: 10.5194/bg-11-6573-2014

Jobbágy, E. G., and Jackson, R. B. (2000). The vertical distribution of soil organic carbon and its relation to climate and vegetation. *Ecol. Appl.* 10, 423–436.

Jones, B. M., Farquharson, L. M., Baughman, C. A., Buzard, R. M., Arp, C. D., Grosse, G., et al. (2018). A decade of remotely sensed observations highlight complex processes linked to coastal permafrost bluff erosion in the Arctic. *Environ. Rese. Lett.* 13:115001. doi: 10.1088/1748-9326/aae471

Juhls, B., Overduin, P. P., Hölemann, J., Hieronymi, M., Matsuoka, A., Heim, B., et al. (2019). Dissolved organic matter at the fluvial–marine transition in the Laptev Sea using in situ data and ocean colour remote sensing. *Biogeosciences* 16, 2693–2713. doi: 10.5194/bg-16-2693-2019

Kaiser, K., and Guggenberger, G. (2000). The role of DOM sorption to mineral surfaces in the preservation of organic matter in soils. *Org. Geochem.* 31, 711–725. doi: 10.1016/S0146-6380(00)00046-2

Kawahigashi, M., Kaiser, K., Rodionov, A., and Guggenberger, G. (2006). Sorption of dissolved organic matter by mineral soils of the Siberian forest tundra. *Glob. Chang. Biol.* 12, 1868–1877. doi: 10.1111/j.1365-2486.2006.01203.x

Kinsey, J. D., Corradino, G., Ziervogel, K., Schnetzer, A., and Osburn, C. L. (2018). Formation of chromophoric dissolved organic matter by bacterial degradation of phytoplankton-derived aggregates. *Front. Mar. Sci.* 4:430. doi: 10.3389/fmars.2017.00430

Köhler, H., Meon, B., Gordeev, V. V., Spitzy, A., and Amon, R. M. W. (2003). "Dissolved organic matter (DOM) in the estuaries of Ob and Yenisei and the adjacent Kara Sea, Russia," in *Proceedings of the Marine Science*, Vol. 6, Amsterdam.

Kovárová-Kovar, K., and Egli, T. (1998). Growth kinetics of suspended microbial cells: from single-substrate-controlled growth to mixed-substrate kinetics. *Microbiol. Mol. Biol. Rev.* 62, 646–666.

Kritzberg, E. S., Duarte, C. M., and Wassmann, P. (2010). Changes in Arctic marine bacterial carbon metabolism in response to increasing temperature. *Polar Biol.* 33, 1673–1682. doi: 10.1007/s00300-010-0799-7

Krzic, M., Watson, K., Grand, S., Bomke, A., Smith, S., Dyanatkar, S., et al. (2010). *Soil Formation and Parent Material. The University of British Columbia, Vancouver, Thompson Rivers University, Kamloops, and Agriculture and Agri-Food Canada, Summerland*. Available online at: https://landscape.soilweb.ca/about/ (accessed November 20, 2020).

Langenheder, S., Kisand, V., Wikner, J., and Tranvik, L. J. (2003). Salinity as a structuring factor for the composition and performance of bacterioplankton degrading riverine DOC. *FEMS Microbiol. Ecol.* 45, 189–202. doi: 10.1016/S0168-6496(03)00149-1

Lawaetz, A. J., and Stedmon, C. A. (2009). Fluorescence intensity calibration using the Raman scatter peak of water. *Appl. Spectrosc.* 63, 936–940. doi: 10.1366/000370209788964548

Lee, S., and Fuhrman, J. A. (1987). Relationships between biovolume and biomass of naturally derived marine bacterioplankton. *Appl. Environ. Microbiol.* 53, 1298–1303. doi: 10.1128/AEM.53.6.1298-1303.1987

Logue, J. B., Stedmon, C. A., Kellerman, A. M., Nielsen, N. J., Andersson, A. F., Laudon, H., et al. (2016). Experimental insights into the importance of aquatic bacterial community composition to the degradation of dissolved organic matter. *ISME J.* 10, 533–545. doi: 10.1038/ismej.2015.131

MacDonald, E. N., Tank, S. E., Kokelj, S. V., Froese, D. G., and Hutchins, R. H. S. (2021). Permafrost-derived dissolved organic matter composition varies across permafrost end-members in the western Canadian Arctic. *Environ. Res. Lett.* 16:024036. doi: 10.1088/1748-9326/abd971

Mann, P. J., Eglinton, T. I., McIntyre, C. P., Zimov, N., Davydova, A., Vonk, J. E., et al. (2015). Utilization of ancient permafrost carbon in headwaters of Arctic fluvial networks. *Nat. Commun.* 6:7856. doi: 10.1038/ncomms8856

Mann, P. J., Spencer, R. G. M., Hernes, P. J., Six, J., Aiken, G. R., Tank, S. E., et al. (2016). Pan-Arctic trends in terrestrial dissolved organic matter from optical measurements. *Front. Earth Sci.* 4:25. doi: 10.3389/feart.2016.00025

Martin, M. (2011). Cutadapt removes adapter sequences from high-throughput sequencing reads. *EMBnet J.* 17:10. doi: 10.14806/ej.17.1.200

Matsuoka, A., Ortega-Retuerta, E., Bricaud, A., Arrigo, K. R., and Babin, M. (2015). Characteristics of colored dissolved organic matter (CDOM) in the Western Arctic Ocean: Relationships with microbial activities. *Deep Sea Res. 2 Top. Stud. Oceanogr.* 118, 44–52. doi: 10.1016/j.dsr2.2015.02.012

McGuire, A. D., Lawrence, D. M., Koven, C., Clein, J. S., Burke, E., Chen, G., et al. (2018). Dependence of the evolution of carbon dynamics in the northern permafrost region on the trajectory of climate change. *Proc. Natl. Acad. Sci. U.S.A.* 115, 3882–3887. doi: 10.1073/pnas.1719903115

Meyers, P. A., and Ishiwatari, R. (1995). "Organic matter accumulation records in lake sediments," in *Physics and Chemistry of Lakes*, eds A. Lerman, D. M. Imboden, and J. R. Gat (Berlin: Springer), 279–328. doi: 10.1007/978-3-642-85132-2_10

Middelboe, M., Glud, R. N., and Sejr, M. K. (2012). Bacterial carbon cycling in a subarctic fjord: a seasonal study on microbial activity, growth efficiency, and virus-induced mortality in Kobbefjord. *Greenland. Limnol. Oceanogr.* 57, 1732–1742. doi: 10.4319/lo.2012.57.6.1732

Miyazaki, M., Nogi, Y., Fujiwara, Y., Kawato, M., Nagahama, T., Kubokawa, K., et al. (2008). *Amphritea japonica* sp. nov. and *Amphritea balenae* sp. nov., isolated from the sediment adjacent to sperm whale carcasses off Kagoshima. *Jpn. Int. J. Syst. Evol. Microbiol.* 58, 2815–2820. doi: 10.1099/ijs.0.65826-0

Moriarty, D. J. W. (1986). "Measurement of bacterial growth rates in aquatic systems from rates of nucleic acid synthesis," in *Advances in Microbial Ecology Advances in Microbial Ecology*, ed. K. C. Marshall (Boston, MA: Springer), 245–292. doi: 10.1007/978-1-4757-0611-6_6

Müller, O., Seuthe, L., Bratbak, G., and Paulsen, M. L. (2018). Bacterial response to permafrost derived organic matter input in an arctic fjord. *Front. Mar. Sci.* 5:263. doi: 10.3389/fmars.2018.00263

Murphy, K. R., Stedmon, C. A., Graeber, D., and Bro, R. (2013). Fluorescence spectroscopy and multi-way techniques. *PARAFAC Anal. Methods* 5:6557. doi: 10.1039/c3ay41160e

Nelson, C. E., and Carlson, C. A. (2012). Tracking differential incorporation of dissolved organic carbon types among diverse lineages of Sargasso Sea bacterioplankton. *Environ. Microbiol.* 14, 1500–1516. doi: 10.1111/j.1462-2920.2012.02738.x

Nelson, C. E., and Wear, E. K. (2014). Microbial diversity and the lability of dissolved organic carbon. *Proc. Natl. Acad. Sci. U.S.A.* 111, 7166–7167. doi: 10.1073/pnas.1405751111

Obu, J., Lantuit, H., Grosse, G., Günther, F., Sachs, T., Helm, V., et al. (2016). Coastal erosion and mass wasting along the Canadian Beaufort Sea based on annual airborne LiDAR elevation data. *Geomorphology* 293, 331–346. doi: 10.1016/j.geomorph.2016.02.014

Obu, J., Westermann, S., Bartsch, A., Berdnikov, N., Christiansen, H. H., Dashtseren, A., et al. (2019). Northern Hemisphere permafrost map based on TTOP modelling for 2000-2016 at 1 km2 scale. *Earth Sci. Rev.* 193, 299–316. doi: 10.1016/j.earscirev.2019.04.023

O'Donnell, J. A., Aiken, G. R., Swanson, D. K., Panda, S., Butler, K. D., and Baltensperger, A. P. (2016). Dissolved organic matter composition of Arctic rivers: linking permafrost and parent material to riverine carbon. *Glob. Biogeochem. Cycles* 30, 1811–1826. doi: 10.1002/2016GB005482

Oksanen, J., Guillaume Blanchet, F., Friendly, M., Kindt, R., Legendre, P., McGlinn, D., et al. (2019). *vegan: Community Ecology Package*. Available online at: https://cran.r-project.org/web/packages/vegan/index.html (accessed May 28, 2020).

Opfergelt, S. (2020). The next generation of climate model should account for the evolution of mineral-organic interactions with permafrost thaw. *Environ. Res. Lett.* 15:091003. doi: 10.1088/1748-9326/ab9a6d

Overeem, I., Anderson, R. S., Wobus, C. W., Clow, G. D., Urban, F. E., and Matell, N. (2011). Sea ice loss enhances wave action at the Arctic coast. *Geophys. Res. Lett.* 38:L17503. doi: 10.1029/2011GL048681

Palmtag, J., and Kuhry, P. (2018). Grain size controls on cryoturbation and soil organic carbon density in permafrost-affected soils. *Permafrost Periglac. Process.* 29, 112–120. doi: 10.1002/ppp.1975

Park, S., Kim, I. K., Lee, J.-S., and Yoon, J.-H. (2019). *Sulfitobacter sabulilitoris* sp. nov., isolated from marine sand. *Int. J. Syst. Evol. Microbiol.* 69, 3230–3236. doi: 10.1099/ijsem.0.003614

Paulsen, M. L., Nielsen, S. E. B., Müller, O., Møller, E. F., Stedmon, C. A., Juul-Pedersen, T., et al. (2017). Carbon bioavailability in a high arctic fjord influenced by glacial meltwater, NE Greenland. *Front. Mar. Sci.* 4:176. doi: 10.3389/fmars.2017.00176

Pollard, W. (2018). "Periglacial processes in glacial environments," in *Past Glacial Environments*, eds J. Menzies and J. J. M. van der Mee (Amsterdam: Elsevier), 537–564. doi: 10.1016/B978-0-08-100524-8.00016-6

Pomeroy, L. R., and Wiebe, W. J. (2001). Temperature and substrates as interactive limiting factors for marine heterotrophic bacteria. *Aquat. Microb. Ecol.* 23, 187–204. doi: 10.3354/ame023187

Quast, C., Pruesse, E., Yilmaz, P., Gerken, J., Schweer, T., Yarza, P., et al. (2013). The SILVA ribosomal RNA gene database project: improved data processing and web-based tools. *Nucleic Acids Res.* 41, D590–D596. doi: 10.1093/nar/gks1219

Rampton, V. N. (1982). *Quaternarygeology of the Yukon Coastal Plain*. Ottawa: Geological Survey of Canada.

Raudina, T. V., Loiko, S. V., Lim, A. G., Krickov, I. V., Shirokova, L. S., Istigechev, G. I., et al. (2017). Dissolved organic carbon and major and trace elements in peat porewater of sporadic, discontinuous, and continuous permafrost zones of western Siberia. *Biogeosciences* 14, 3561–3584. doi: 10.5194/bg-14-3561-2017

Robinson, M. D., and Smyth, G. K. (2008). Small-sample estimation of negative binomial dispersion, with applications to SAGE data. *Biostatistics* 9, 321–332. doi: 10.1093/biostatistics/kxm030

Robinson, M. D., McCarthy, D. J., and Smyth, G. K. (2010). edgeR: a Bioconductor package for differential expression analysis of digital gene expression data. *Bioinformatics* 26, 139–140. doi: 10.1093/bioinformatics/btp616

Romanenko, L. A., Tanaka, N., Svetashev, V. I., and Kalinovskaya, N. I. (2011). *Pacificibacter maritimus* gen. nov., sp. nov., isolated from shallow marine sediment. *Int. J. Syst. Evol. Microbiol.* 61, 1375–1381. doi: 10.1099/ijs.0.026047-0

Romanovsky, V. E., Smith, S. L., and Christiansen, H. H. (2010). Permafrost thermal state in the polar Northern Hemisphere during the international polar year 2007-2009: a synthesis. *Permafrost Periglac. Process.* 21, 106–116. doi: 10.1002/ppp.689

Rosenstock, B., and Simon, M. (2001). Sources and sinks of dissolved free amino acids and protein in a large and deep mesotrophic lake. *Limnol. Oceanogr.* 46, 644–654. doi: 10.4x319/lo.2001.46.3.0644

Ruiz-González, C., Niño-García, J. P., and Del Giorgio, P. A. (2015). Terrestrial origin of bacterial communities in complex boreal freshwater networks. *Ecol. Lett.* 18, 1198–1206. doi: 10.1111/ele.12499

Schirrmeister, L., Grosse, G., Wetterich, S., Overduin, P. P., Strauss, J., Schuur, E. A. G., et al. (2011). Fossil organic matter characteristics in permafrost deposits of the northeast Siberian Arctic. *J. Geophys. Res.* 116:G00M02. doi: 10.1029/2011JG001647

Schnetger, B., and Lehners, C. (2014). Determination of nitrate plus nitrite in small volume marine water samples using vanadium(III)chloride as a reduction agent. *Mar. Chem.* 160, 91–98. doi: 10.1016/j.marchem.2014.01.010

Schuur, E. A. G., McGuire, A. D., Schädel, C., Grosse, G., Harden, J. W., Hayes, D. J., et al. (2015). Climate change and the permafrost carbon feedback. *Nature* 520, 171–179. doi: 10.1038/nature14338

Semiletov, I. P., Shakhova, N. E., Pipko, I. I., Pugach, S. P., Charkin, A. N., Dudarev, O. V., et al. (2013). Space-time dynamics of carbon and environmental parameters related to carbon dioxide emissions in the Buor-Khaya Bay and adjacent part of the Laptev Sea. *Biogeosciences* 10, 5977–5996. doi: 10.5194/bg-10-5977-2013

Sipler, R. E., Kellogg, C. T. E., Connelly, T. L., Roberts, Q. N., Yager, P. L., and Bronk, D. A. (2017). Microbial community response to terrestrially derived dissolved organic matter in the coastal arctic. *Front. Microbiol.* 8:1018. doi: 10.3389/fmicb.2017.01018

Sjöstedt, J., Hagström, Å, and Zweifel, U. L. (2012a). Variation in cell volume and community composition of bacteria in response to temperature. *Aquat. Microb. Ecol.* 66, 237–246. doi: 10.3354/ame01579

Sjöstedt, J., Koch-Schmidt, P., Pontarp, M., Canbäck, B., Tunlid, A., Lundberg, P., et al. (2012b). Recruitment of members from the rare biosphere of marine bacterioplankton communities after an environmental disturbance. *Appl. Environ. Microbiol.* 78, 1361–1369. doi: 10.1128/AEM.05542-11

Smith, S. L., Romanovsky, V. E., Lewkowicz, A. G., Burn, C. R., Allard, M., Clow, G. D., et al. (2010). Thermal state of permafrost in North America: a contribution to the international polar year. *Permafrost Periglac. Process.* 21, 117–135. doi: 10.1002/ppp.690

Sorokin, D. Y. (1995). *Sulfitobacter pontiacus* gen. nov., sp. nov. — A new heterotrophic bacterium from the black sea, specialized on sulfite oxidation. *Mikrobiologiya* 64:295.

Spencer, R. G. M., Mann, P. J., Dittmar, T., Eglinton, T. I., McIntyre, C., Holmes, R. M., et al. (2015). Detecting the signature of permafrost thaw in Arctic rivers. *Geophys. Res. Lett.* 42, 2830–2835. doi: 10.1002/2015GL063498

Stapel, J. G., Schwamborn, G., Schirrmeister, L., Horsfield, B., and Mangelsdorf, K. (2017). Substrate potential of last interglacial to Holocene permafrost organic matter for future microbial greenhouse gas production. *Biogeosciences* 15, 1969–1985. doi: 10.5194/bg-15-1969-2018

Stedmon, C. A., and Nelson, N. B. (2015). "The optical properties of DOM in the ocean," in *Biogeochemistry of Marine Dissolved Organic Matter*, eds D. A. Hansell and C. A. Carlson (Amsterdam: Elsevier), 481–508. doi: 10.1016/B978-0-12-405940-5.00010-8

Strauss, J., Schirrmeister, L., Grosse, G., Fortier, D., Hugelius, G., Knoblauch, C., et al. (2017). Deep Yedoma permafrost: a synthesis of depositional characteristics and carbon vulnerability. *Earth Sci. Rev.* 172, 75–86. doi: 10.1016/j.earscirev.2017.07.007

Svoboda, P., Lindström, E. S., Ahmed Osman, O., and Langenheder, S. (2018). Dispersal timing determines the importance of priority effects in bacterial communities. *ISME J.* 12, 644–646. doi: 10.1038/ismej.2017.180

Tank, S. E., Vonk, J. E., Walvoord, M. A., McClelland, J. W., Laurion, I., and Abbott, B. W. (2020). Landscape matters: predicting the biogeochemical effects of permafrost thaw on aquatic networks with a state factor approach. *Permafrost Periglac. Process.* 31, 358–370. doi: 10.1002/ppp.2057

Tanski, G., Couture, N., Lantuit, H., Eulenburg, A., and Fritz, M. (2016). Eroding permafrost coasts release low amounts of dissolved organic carbon (DOC) from ground ice into the nearshore zone of the Arctic Ocean. *Glob. Biogeochem. Cycles* 30, 1054–1068. doi: 10.1002/2015GB005337

Tanski, G., Wagner, D., Knoblauch, C., Fritz, M., Sachs, T., and Lantuit, H. (2019). Rapid co_2 release from eroding permafrost in seawater. *Geophys. Res. Lett.* 46, 11244–11252. doi: 10.1029/2019GL084303

Textor, S. R., Guillemette, F., Zito, P. A., and Spencer, R. G. M. (2018). An assessment of dissolved organic carbon biodegradability and priming in blackwater systems. *J. Geophys. Res. Biogeosci.* 123, 2998–3015. doi: 10.1029/2018JG004470

Textor, S. R., Wickland, K. P., Podgorski, D. C., Johnston, S. E., and Spencer, R. G. M. (2019). Dissolved organic carbon turnover in permafrost-influenced watersheds of interior alaska: molecular insights and the priming effect. *Front. Earth Sci.* 7:275. doi: 10.3389/feart.2019.00275

Thingstad, T. F., Bellerby, R. G. J., Bratbak, G., Børsheim, K. Y., Egge, J. K., Heldal, M., et al. (2008). Counterintuitive carbon-to-nutrient coupling in an Arctic pelagic ecosystem. *Nature* 455, 387–390. doi: 10.1038/nature07235

Thomas, F., Hehemann, J.-H., Rebuffet, E., Czjzek, M., and Michel, G. (2011). Environmental and gut bacteroidetes: the food connection. *Front. Microbiol.* 2:93. doi: 10.3389/fmicb.2011.00093

Van der Gucht, K., Cottenie, K., Muylaert, K., Vloemans, N., Cousin, S., Declerck, S., et al. (2007). The power of species sorting: local factors drive bacterial community composition over a wide range of spatial scales. *Proc. Natl. Acad. Sci. U.S.A.* 104, 20404–20409. doi: 10.1073/pnas.0707200104

Vannote, R. L., Minshall, G. W., Cummins, K. W., Sedell, J. R., and Cushing, C. E. (1980). The river continuum concept. *Can. J. Fish. Aquat. Sci.* 37, 130–137. doi: 10.1139/f80-017

Vonk, J. E., Mann, P. J., Davydov, S., Davydova, A., Spencer, R. G. M., Schade, J., et al. (2013). High biolability of ancient permafrost carbon upon thaw. *Geophys. Res. Lett.* 40, 2689–2693. doi: 10.1002/grl.50348

Vonk, J. E., Sánchez-García, L., van Dongen, B. E., Alling, V., Kosmach, D., Charkin, A., et al. (2012). Activation of old carbon by erosion of coastal and subsea permafrost in Arctic Siberia. *Nature* 489, 137–140. doi: 10.1038/nature11392

Vonk, J. E., Tank, S. E., Bowden, W. B., Laurion, I., Vincent, W. F., Alekseychik, P., et al. (2015). Reviews and syntheses: effects of permafrost thaw on Arctic aquatic ecosystems. *Biogeosciences* 12, 7129–7167. doi: 10.5194/bg-12-7129-2015

Walker, S. A., Amon, R. M. W., and Stedmon, C. A. (2013). Variations in high-latitude riverine fluorescent dissolved organic matter: a comparison of large Arctic rivers. *J. Geophys. Res. Biogeosci.* 118, 1689–1702. doi: 10.1002/2013JG002320

Walter Anthony, K., Schneider von Deimling, T., Nitze, I., Frolking, S., Emond, A., Daanen, R., et al. (2018). 21st-century modeled permafrost carbon emissions accelerated by abrupt thaw beneath lakes. *Nat. Commun.* 9:3262. doi: 10.1038/s41467-018-05738-9

Wang, Y., Naumann, U., Wright, S. T., and Warton, D. I. (2012). mvabund - anR package for model-based analysis of multivariate abundance data. *Methods Ecol. Evol.* 3, 471–474. doi: 10.1111/j.2041-210X.2012.00190.x

Ward, C. P., and Cory, R. M. (2015). Chemical composition of dissolved organic matter draining permafrost soils. *Geochim. Cosmochim. Acta* 167, 63–79. doi: 10.1016/j.gca.2015.07.001

Weishaar, J. L., Aiken, G. R., Bergamaschi, B. A., Fram, M. S., Fujii, R., and Mopper, K. (2003). Evaluation of specific ultraviolet absorbance as an indicator of the chemical composition and reactivity of dissolved organic carbon. *Environ. Sci. Technol.* 37, 4702–4708. doi: 10.1021/es030360x

Wickland, K. P., Waldrop, M. P., Aiken, G. R., Koch, J. C., Jorgenson, M. T., and Striegl, R. G. (2018). Dissolved organic carbon and nitrogen release from boreal Holocene permafrost and seasonally frozen soils of Alaska. *Environ. Res. Lett.* 13:065011. doi: 10.1088/1748-9326/aac4ad

Wild, B., Andersson, A., Bröder, L., Vonk, J., Hugelius, G., McClelland, J. W., et al. (2019). Rivers across the Siberian Arctic unearth the patterns of carbon release from thawing permafrost. *Proc. Natl. Acad. Sci. U.S.A.* 116, 10280–10285. doi: 10.1073/pnas.1811797116

Wologo, E., Shakil, S., Zolkos, S., Textor, S., Ewing, S., Klassen, J., et al. (2020). Stream dissolved organic matter in permafrost regions shows surprising compositional similarities but negative priming and nutrient effects. *Glob. Biogeochem. Cycles* 35:e2020GB006719. doi: 10.1029/2020GB006719

Wolter, J., Lantuit, H., Herzschuh, U., Stettner, S., and Fritz, M. (2017). Tundra vegetation stability versus lake-basin variability on the Yukon Coastal Plain (NW Canada) during the past three centuries. *Holocene* 27, 1846–1858. doi: 10.1177/0959683617708441

Yamashita, Y., and Tanoue, E. (2003). Chemical characterization of protein-like fluorophores in DOM in relation to aromatic amino acids. *Mar. Chem.* 82, 255–271. doi: 10.1016/S0304-4203(03)00073-2

Yoon, J.-H., Kang, S.-J., and Oh, T.-K. (2005). *Marinomonas dokdonensis* sp. nov., isolated from sea water. *Int. J. Syst. Evol. Microbiol.* 55, 2303–2307. doi: 10.1099/ijs.0.63830-0

Zhang, D.-C., Li, H.-R., Xin, Y.-H., Liu, H.-C., Chen, B., Chi, Z.-M., et al. (2008). *Marinomonas arctica* sp. nov., a psychrotolerant bacterium isolated from the Arctic. *Int. J. Syst. Evol. Microbiol.* 58, 1715–1718. doi: 10.1099/ijs.0.65737-0

Zhang, Z., Qin, J., Sun, H., Yang, J., and Liu, Y. (2020). Spatiotemporal dynamics of dissolved organic carbon and freshwater browning in the Zoige Alpine Wetland, Northeastern Qinghai-Tibetan Plateau. *Water* 12:2453. doi: 10.3390/w12092453

Zweifel, U. L., Blackburn, N., and Hagström, Å (1996). Cycling of marine dissolved organic matter. I. An experimental system. *Aquat. Microb. Ecol.* 11, 65–77. doi: 10.3354/ame011065

Conflict of Interest: The authors declare that the research was conducted in the absence of any commercial or financial relationships that could be construed as a potential conflict of interest.